Unimolecular dissociation characteristics of cationic complexes between nicotinic acid and Cu(II) and Ni(II)

Héloïse Dossmann, Carlos Afonso, Jean-Claude Tabet, Einar Uggerud

Unimolecular dissociation characteristics of cationic complexes between nicotinic acid and Cu(II) and Ni(II)*

Héloïse Dossmann,[a] Carlos Afonso,[a.b] Jean-Claude Tabet[a] and Einar Uggerud[c]

[a] Institut Parisien de Chimie Moléculaire. Université Pierre et Marie Curie-Paris 6. UMR 7201- FR2769. Place Jussieu. F-75252 Paris Cedex 05. France. [b] Université de Rouen. UMR CNRS 6014 COBRA. 1 rue Tesnière. 76130 Mont-Saint-Aignan. France and [c] Massespektrometrilaboratoriet og Senter for teoretisk og beregningsbasert kjemi (CTCC). Kjemisk institutt. Universitetet i Oslo. Postboks 1033 Blindern. N-0315 Oslo. Norway. E-mail: heloise.dossmann@upmc.fr or einar.uggerud@kjemi.uio.no

Highlights

1. We have formed and characterized $ML(L\text{-}H)^+$ complexes
2. We find preference for metal coordination by the carboxylate group
3. Collisionally-induced dissociation gives CO_2 loss as the primary product
4. The dissociation patterns are consistent with the known chemistry of Cu^{2+} and Ni^{2+}

Abstract

Cu^{2+} and Ni^{2+} form dimeric $ML(L\text{-}H)^+$ complexes with nicotinic acid (M = Cu, Ni; L = nicotinic acid) upon electrospray ionization. Quantum chemical calculations indicate thermochemical preference for coordination of the carboxylate groups rather than the ring nitrogens to the central metal ion in both cases. In analogy to the dimeric metal complexes of amino acids the primary dissociation reaction upon collisional activation of $ML(L–H)^+$ is the loss of CO_2 in both cases. Further dissociation of the decarboxylated species show preference for loss of a 3-pyridinyl radical for M = Cu and $NiCO_2$ for M = Ni. This can be understood in light of the redox properties of the two metals and from previous studies of similar complexes with amino acids. Loss of the pyridinyl radical bonded to the carboxylate group in these cationic entities does not lead to $M(\eta^2\text{-}O_2C)$ structures previously observed for similar anionic metal species.

Key words

Organometallic chemistry, reactivity, mass spectrometry, CO_2 activation, decarboxylation

---

*) Dedicated to the memory of Detlef Schröder.

Graphical abstract

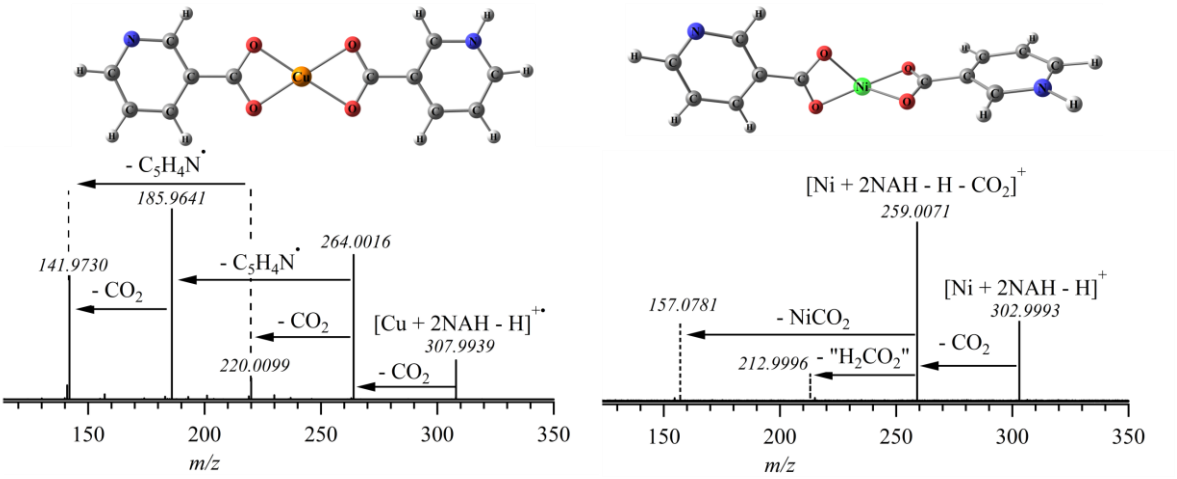

Introduction

Recently, a new bidentate structural binding motif of carbon dioxide to various metals and metal ions has been described.[1-4] Such tetragonal structures (Scheme 1) can be formed by electrospray ionization (ESI) of liquids containing suitable precursor compounds in combination with collisional activation and have very interesting chemical properties. For example $XMg(\eta^2\text{-}O_2C)^-$ (X= Cl, Br or OH) formed from mixtures of MgX_2 salts and oxalic acid has been shown to be a carbon nucleophile and may serve as a model system for carbon dioxide activation during organic and biological C–C bond formation reactions, for example during photosynthesis. Carboxylation reactions of this kind are of significant current interest as a promising method for CO_2 sequestration in industrial processes for combined combustion and chemical synthesis.[5] In this respect it is of great interest to investigate how chemical factors (the metal, the charge state, complexation and solvent) influence the stability of this binding motif. In our quest for suitable model systems of this kind we have chosen a simple strategy, namely to mix a salt of the metal in question with carboxylic acids and study the collisionally-induced decomposition of the ionic complexes formed in situ in the electrospray process. In the present context we chose to study the M(II) salts of nickel and copper, since they are among the most interesting metals both for industrial catalysis and in biological systems. On the other hand, copper and nickel have quite different redox properties. While copper normally displays oxidation state 0, I and II, oxidation state I is rare for nickel. The former metal is characterized for its flexibility in oxygen processing and radical initiated processes, the latter by its catalytic role in hydrogenation/dehydrogenation reactions (Raney nickel) and in C–C activation.

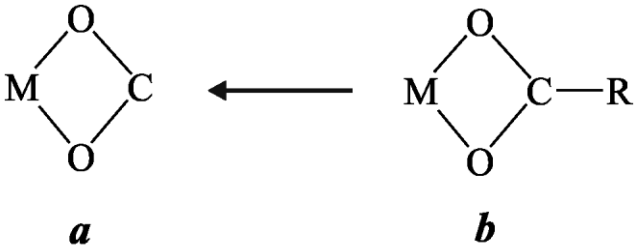

Scheme 1.

The simplest conceivable Cu^{2+} and Ni^{2+} complex structures formed with carboxylates are of the type $(R\text{-}CO_2)_2M$, providing a conceptual starting point for forming precursors that by direct loss of R may lead to structures of the type $(R\text{-}CO_2)M(\eta^2\text{-}O_2C)$ upon activation, see Scheme 1. In order to form positively charged ions of such $(R\text{-}CO_2)_2M$ complexes by ESI it is necessary that the ligand in addition to a carboxylic acid residue also contains a sufficiently basic site, for example an amino group to pick up an extra proton. On the other hand, amino groups also have affinity for cationic transition metal ions so within the ligand there will be competition between metal complexation of the carboxylate and the amino groups, leading to structural complexity. This is a well-known situation for amino acids, which give rise to various monomeric, dimeric and trimeric complexes with both copper and nickel in ESI mass

spectrometry, and the unimolecular dissociation of Cu(II) amino acid and carboxylic acid complexes has been particularly well studied by mass spectrometry due to the rich radical cation chemistry resulting from the open shell d^9 electronic configuration of Cu^{2+}.[6-12] On the other hand Ni^{2+} is d^8, an even electron species with lower tendency towards radical chemistry.[13-15]

The structural flexibility of amino acids allows for strong interaction between the metal ion and several functional groups of the ligand. To overcome this issue we decided to investigate complexes of nicotinic acid since this ligand is both simpler and more rigid than amino acids, avoiding simultaneous binding to the nitrogen and the carboxylic acid/carboxylate group of the same ligand molecule to the metal. Different mass spectrometric approaches have been used in order to determine the binding patterns of the formed complexes as well as their dissociation behaviour. These efforts were complemented by density functional theory (DFT)-based calculations.

Methods

Experimental details

General

All chemicals have been purchased from Sigma–Aldrich (St. Quentin Fallavier, France) and used without further purification. 40 µM solutions of MCl_2 (M = Cu, Ni) and nicotinic acid were prepared in methanol. Working solutions were prepared by mixing these two solutions in a 5:1 ratio (v:v).

Ion trap

Experiments were in part performed on a quadrupole ion trap mass spectrometer (Esquire 3000, Bruker, Bremen, Germany) equipped with an orthogonal ESI source. Sample solutions were infused with a syringe pump model 74900 (Cole-Parmer. Vernon Hills. IL) at a flow rate of 160 µL h^{-1}. Nitrogen was used as nebulizing gas at a pressure of 6 psi, and as drying gas at a temperature of 250 °C and a flow rate of 4 L min^{-1}. Optimized source voltages were as followed: capillary at −3.5 kV, end plate offset at −500 V, capillary exit (CE) at +45 V, skimmer 1 at +15 V (providing a potential difference of 30 V with CE), and skimmer 2 at +6 V. These relatively soft source conditions were used in order to preserve the rather weakly complexed ions. The low mass cut-off (LMCO) was fixed at 28% of the *m/z* of the precursor ions and the analytical scan range for mass spectra was *m/z* 50–600. The scan rate was set at 13.000 *m/z* s^{-1} (standard mode). Ion accumulation time was automatically set with ion charge control (ICC) with a target of 10.000 to limit space charge effects. For low-energy sequential collisionally-induced dissociation (CID) experiments, resonant excitation was used with an amplitude voltage of 0.70 V_{p-p} and an ion isolation window of *m/z* 0.8 in order to obtain monoisotopic ion selection.

FT-ICR

A hybrid quadrupole Fourier transform ion cyclotron resonance (hQh-FT/ICR) mass spectrometer (Solarix, Bruker Daltonics, Bremen, Germany) equipped with an actively

shielded 7 T was used for accurate mass measurements. The samples were infused in the electrospray ion source at a flow rate of 120 μL h^{-1} with the assistance of N_2 nebulizing gas. Ionization was performed in the positive ion mode with an ESI high voltage of 4000 V. Voltage applied in the desolvation zone were: capillary exit 200 V, deflector 180 V, funnel 110 V, skimmer 50 V. Complexes of interest were first mass-selected with the quadrupole (*m/z* 5 window), accumulated for 0.5 s in a linear ion trap and then isolated in the ICR cell in order to obtain monoisotopic precursor ion selection (13 % of frequency sweep amplitude). Activation of the ions was performed using sustained off-resonance irradiation collision-induced dissociations (SORI-CID) using argon as collision gas introduced through a pulse valve. The ions were excited using excitation amplitude of 0.5 V_{p-p} with a frequency offset of -500 Hz applied for 200 ms. A pumping delay of 2 s was used before the excitation/detection step.

All mass spectra and collision activation spectra were acquired with Solarix control (version 1.5. Bruker Daltonics) in broadband mode from *m/z* 21.5 to *m/z* 500. The image signal was amplified and digitized using 2M data point resulting in the recording of a 0.4 s time domain which was transformed into the corresponding frequency domain by Fourier transform (one zero fill and apodization using the sinbell function).

The ESI mass spectra were internally calibrated from unambiguous signals (single point calibration). Typically the precursor ion was used as internal calibrant for CID spectra. Reported *m/z* ions were compared to the theoretical *m/z* and ions with an error higher than 5 ppm were not considered.

Ion mobility measurements

The ion mobility experiments were carried out using a Synapt G2 HDMS (Waters, Manchester, United Kingdom). This instrument is a hybrid quadrupole/time-of-flight mass spectrometer, which incorporates a traveling-wave ion mobility (TWIM) device, in which low-voltage waves push the ions through a gas filled cell.[16] The gas flow (N_2) was set at 90 mL min^{-1}, the traveling wave height and velocity were set to 40 V and 600 m s^{-1}, respectively. For comparison, theoretical collision cross section values were computed using the trajectory method (TM) method with the MOBCAL software.[17, 18] The number of data points in the Monte Carlo integrations of impact parameter and orientation was set to 1000. IMS cell calibration was carried out with polyalanines at the concentration of 10 ng μL^{-1} using collision cross section (CCS) values used for calibration from the Clemmer lab database.[19]

Computational procedure

Quantum chemical calculations were carried out using the program system GAUSSIAN 09.[20] Geometry optimization and single point energies were obtained using the B3LYP method with the 6-31G(2df,p) basis set. All structures presented in this work were characterised either as minima or saddle points from vibrational analysis. Relative energies were corrected by including unscaled zero-point vibrational energies (ZPVE). The accuracy of the computational approach was probed by comparing calculated bond dissociation energies of selected copper and nickel complexes with experimental values found in the

literature. The results show satisfying agreement and are presented in the Supplementary information.

Results

Electrospray spectra

The positive mode ESI mass spectra of the MCl_2/nicotinic acid solutions display significant peaks corresponding to $ML(L–H)^+$ and $ML_2(L–H)^+$ (M = Cu, Ni; L = nicotinic acid) in agreement with the theoretical isotope masses and distributions. Depending on the nicotinic acid concentration, we also observe the protonated monomer and dimers of nicotinic acid. At higher concentrations of $CuCl_2$, we also identify a peak corresponding to $Cu_2L(L–H)^{+\bullet}$. The metal complexes were also seen to form mono-adducts with methanol from the solvent.

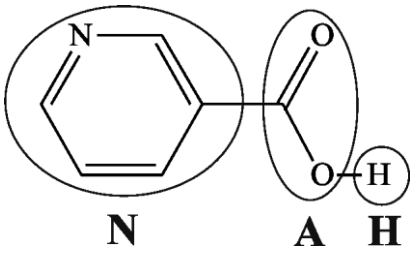

Scheme 2.

Binding patterns in the neat cluster ions, computational insight

In the present context, the molecular structures of the $ML(L–H)^+$ ions (M = Cu, Ni) are of key interest. Nicotinic acid (L) and its anion $(L–H)^–$ allow for various binding patterns, and the question arises whether there is preference for binding the ligand L = NAH to the metal core via the ring nitrogen (N side) or the carboxylic acid/carboxylate group (A side), see Scheme 2. To investigate this we conducted quantum chemical calculations for all isomeric forms obtained by varying the complexation site (N or A) in both ligands and by varying the position of the movable proton (N or A in both ligands). We also noted that the molecular geometry of nicotinic acid does not allow for simultaneous binding of both N and A to the metal, avoiding a complicating factor in more flexible molecules containing the same functional groups (amino acids, peptides etc.). For both copper and nickel we find that the lowest energy forms correspond to tetradendate carboxylate arrangements $NA\text{-}M\text{-}ANH^+$, in which the non-deprotonated ligand exists in its zwitterionic form, *i.e.* the moveable proton resides on one of the non-metalbonding nitrogen atoms. The situations are depicted in Figure 1 and 2, which also show that the copper(II) complex is square planar while the nickel(II) complex is tetrahedral in the most stable triplet electronic configuration, in good agreement with previous observations.[21, 22] The latter may also exist in a low-lying singlet state (14 kJ $mol^{–1}$ higher than the triplet), for which the square planar arrangement is preferred.

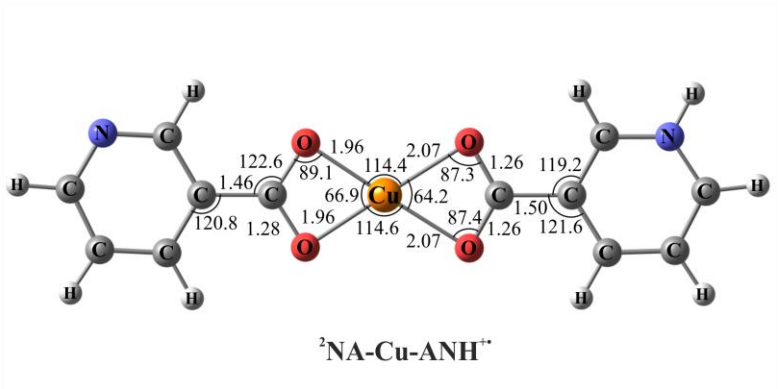

Figure 1. Geometry optimized structure of the most stable [Cu + 2NAH – H]$^{+\bullet}$ complexes (doublet). Bond lengths are in Å and angles in degrees.

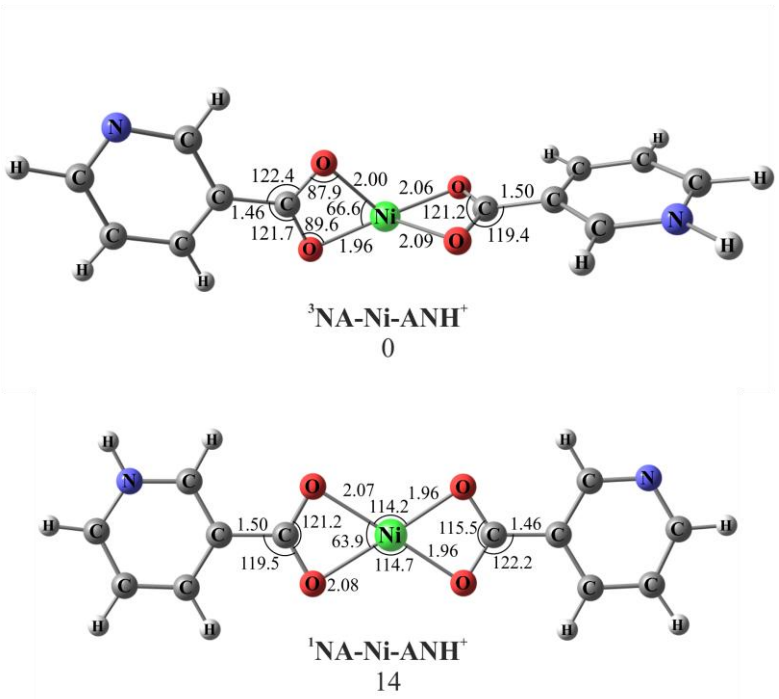

Figure 2. Geometry optimized structures of the two most stable [Ni + 2NAH – H]$^{+}$ complexes (triplet and singlet). Relative energies are in kJ mol^{-1}, bond lengths in Å and angles in degrees.

A fuller account of the relative energies of possible isomeric forms is given in the Supplementary information, which shows that the forms where nitrogen is coordinated to the metal, as in (AN-M-ANH^{+}) and (AN-M-NAH^{+}), are clearly lower in energy for copper than for nickel.

Ion mobility measurements

As outlined above, the [M + 2NAH – H]$^{+}$ complexes (M = Cu, Ni) may present different binding patterns. To probe whether only one isomer is preferentially formed or a mixture of different isomers is present in the electrospray, we conducted ion mobility measurements (Figure S1 and Table 1). Experimental collision cross sections of the detected ions were determined from travelling wave ion mobility experiments. However, in most experiments

only one isomeric species could be resolved, but a minor isomeric complex (6.6 %) was evidenced for the $CuL(L–H)^{+\bullet}$ ion (*m/z* 308) with a drift time of 2.46 ms (94 $Å^2$). The main $CuL(L–H)^{+\bullet}$ copper dimer (100 %) was detected with a drift time of 2.68 ms (100.3 $Å^2$) and the $NiL(L–H)^+$ nickel dimer presented a drift time of 2.72 ms (101.4 $Å^2$) (Table 1).

Table 1. Experimental collision cross sections (CCS) (polyAla calibration) obtained for $[M + 2NAH – H]^+$ complexes (M = Cu, Ni)

Ion	**Drift time (ms)**	**CCS ($Å^2$)**
$[2NAH – H + Cu]^{+\bullet}$	2.46	94.0
$[2NAH – H + Cu]^{+\bullet}$	2.68	100.3
$[2NAH – H + Ni]^+$	2.72	101.4

Table 2. Theoretical CCS determination of the two most stable calculated forms of each $[M + 2NAH – H]^+$ complex (M = Cu, Ni)

Ion	**CCS ($Å^2$)**
$^2NA\text{-}Cu\text{-}ANH^{+\bullet}$	102.1
$^2NA\text{-}Cu\text{-}NAH^{+\bullet}$	102.2
$^1NA\text{-}Ni\text{-}ANH^+$	101.0
$^3NA\text{-}Ni\text{-}ANH^+$	102.3

The calculated CCS values for the optimized geometries were determined using the trajectory method (Table 2). The obtained values are consistent with the corresponding experimental values for both nickel and copper complexes (Table 1). However, on the basis of the very similar cross sections of the isomeric structures located in quantum chemical calculations study, one would in hindsight not expect them to be separable in the ion mobility experiment. On the other hand, the minor isomeric copper dimer with an experimental CCS of 94 $Å^2$ must have a significantly more compact structure. Unfortunately, the quantum chemical calculations could not help us in identifying this more compact structure. CID experiments performed subsequent to the ion mobility separation showed that this minor component is significantly more fragile towards dissociation than the major component (data not shown), thereby indicating lower thermochemical stability.

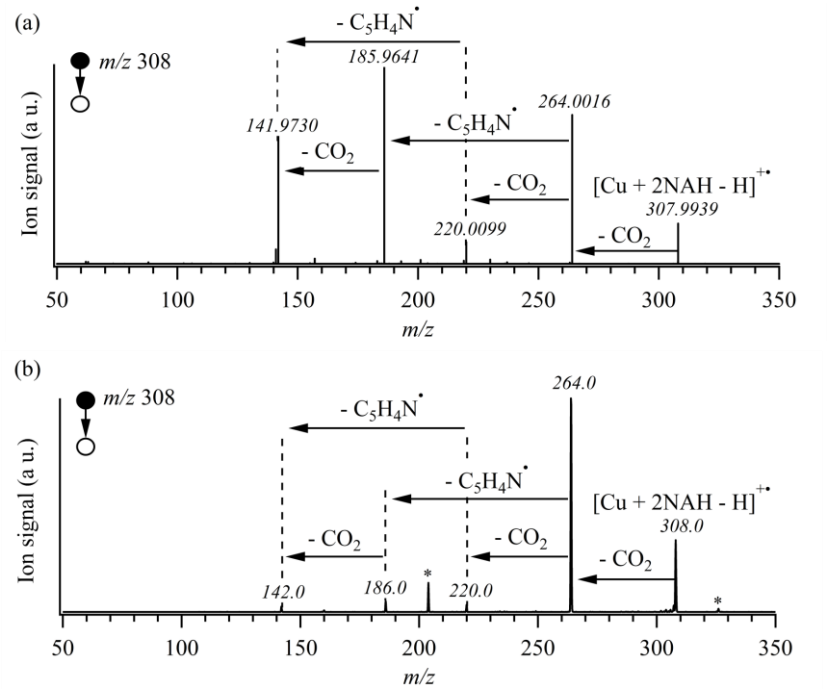

Figure 3. MS^2 (a) SORI-CID (FT-ICR) and (b) CID (ion trap) spectra of $[Cu + 2NAH - H]^{+\bullet}$ (*m/z* 308). In spectrum (b), some ions have captured a water molecule due to the presence of water in the trap. These water adducts are indicate by an asterisk.

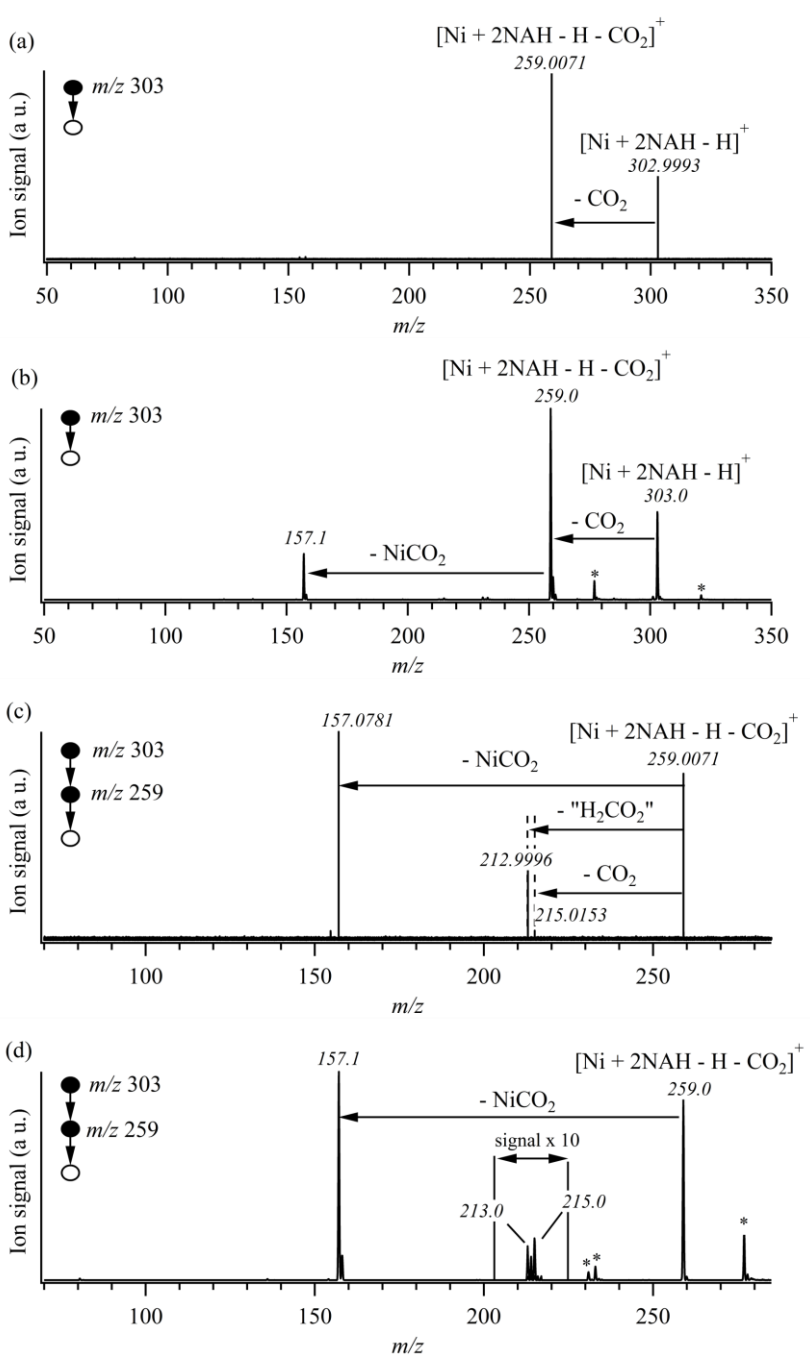

Figure 4. MS^2- (a) SORI-CID (FT-ICR) and (b) CID (ion trap) spectra of $[Ni + 2NAH – H]^+$ (*m/z* 303) and MS^3 (c) SORI-CID and (d) CID spectra of $[Ni + 2NAH – H – CO_2]^+$ (*m/z* 259). In spectra (b) and (d), some ions have captured a water molecule due to the presence of water in the trap. These water adducts are indicate by an asterisk.

Dissociation of $[M + 2NAH – H]^+$ complexes (M = Cu, Ni)

Activation of $[M + 2NAH – H]^+$ complexes (M = Cu, Ni) was done using two activation methods. The first, low-energy CID experiments, was performed on a quadruple ion trap and the second, SORI-CID activation, was carried out on a FT-ICR mass spectrometer. When the former gives usually access to the lower energy dissociation pathways,[23] the latter is known to enable slow fragmentation processes, which may sometimes not be entropically favourable.

In fact, both techniques are considered as slow heating methods,[24] the main differences is the high pressure conditions of the quadrupole ion trap yielding a fast cooling of the ions which limits consecutive dissociation and favour the low energy dissociation pathways.[23] For the FT-ICR, because of the low-pressure condition no collisional cooling of the product ions is expected yielding low kinetic shift.[12, 25] Hence, comparing these two activation spectra may bring some information concerning the dissociation processes observed.

The dominating dissociation reaction observed for both $[Cu + 2NAH – H]^{+\bullet}$ (m/z 303) and $[Ni + 2NAH – H]^{+}$ (*m/z* 308) is the loss of a single CO_2 molecule, leading to $[M + 2NAH – H – CO_2]$+. This is confirmed from the FT-ICR (SORI-CID) and ion trap experiments (Figures 3 and 4). The decarboxylated fragment ions $[M + 2NAH – H – CO_2]^{+}$ (M = Cu, Ni) may fragment further but now reflecting the influence of the metal centre. While the decarboxylated species may lose a second molecule of CO_2 for both M = Cu and Ni (Figure 3 and 4c), the dominating secondary reaction for M = Ni is loss of $NiCO_2$ while it is loss of the ring fragment radical $C_5H_4N^{\bullet}$ for M = Cu. The latter corresponds to the dissociation pattern seen for amino acid copper(II) complexes of the same kind, described in great detail in the literature.[9] For $[Cu + 2NAH – H – CO_2]^{+\bullet}$ we also note the loss of $CO_2 + C_5H_4N^{\bullet}$. All these observations are verified by accurate mass measurements. The SORI-CID spectrum of $[Ni + 2NAH – H – CO_2]^{+}$, Figure 4c, also shows a peak for loss of CH_2O_2, probably either due to the successive H_2O and CO losses or loss of formic acid. This is clearly a relatively high-energy process since it is not seen in the low energy collision spectra (ion trap), in analogy with previous observations by Bouchonnet et al. for complexes between Cu(II) and amino acids.[8]

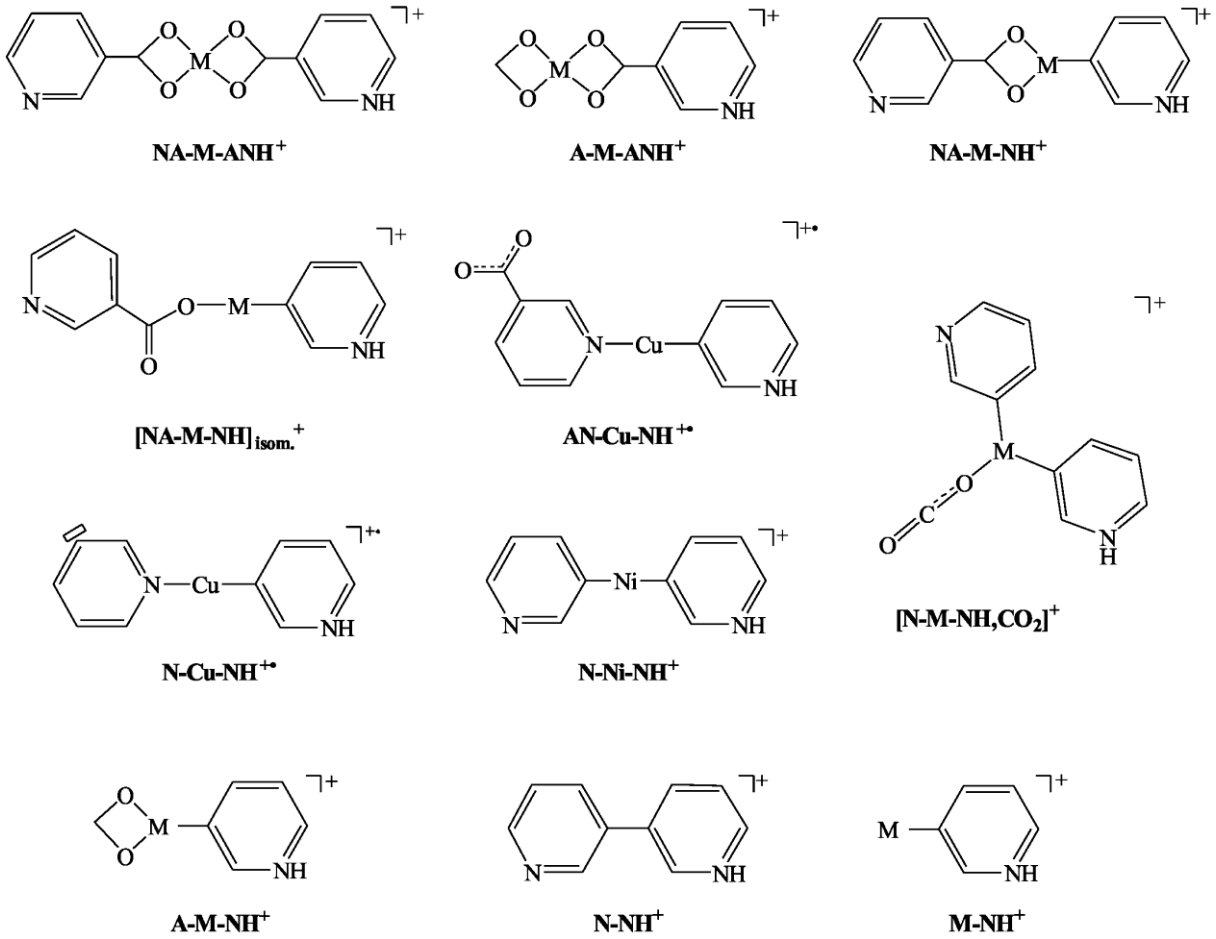

Scheme 3.

Dissociation mechanisms

Possible dissociation pathways were investigated by means of quantum chemical calculations. For the sake of clarity, we only present schematic representation of involved ion structures (Scheme 3) and geometries of transition structures here (Figures 6 and 8). Optimized geometries and energies for all calculated structures are presented in Supplementary information.

A schematic potential energy diagram based on the quantum chemical calculations for [Cu + 2NAH – H]$^{+\bullet}$ is reproduced in Figure 5. Several pathways may lead to the same product pairs (or isomeric product pairs) but only the lowest energy route for each process is indicated to keep the diagram simple. The diagram shows that the facile decarboxylation reaction may occur directly from the square planar global potential energy minimum NA-Cu-ANH$^{+\bullet}$ by a C–C bond activation mechanism involving partial rotation of the protonated ligand ANH, thereby liberating the carboxylate in the form of CO_2 from the metal centre via **TS$_{Cu}$1** (Figure 6). This rearrangement/dissociation mechanism leads to NA-Cu-NH$^{+\bullet}$ at 44 kJ mol^{-1}, in which the carbon of the remaining NH unit is bonded directly to Cu.

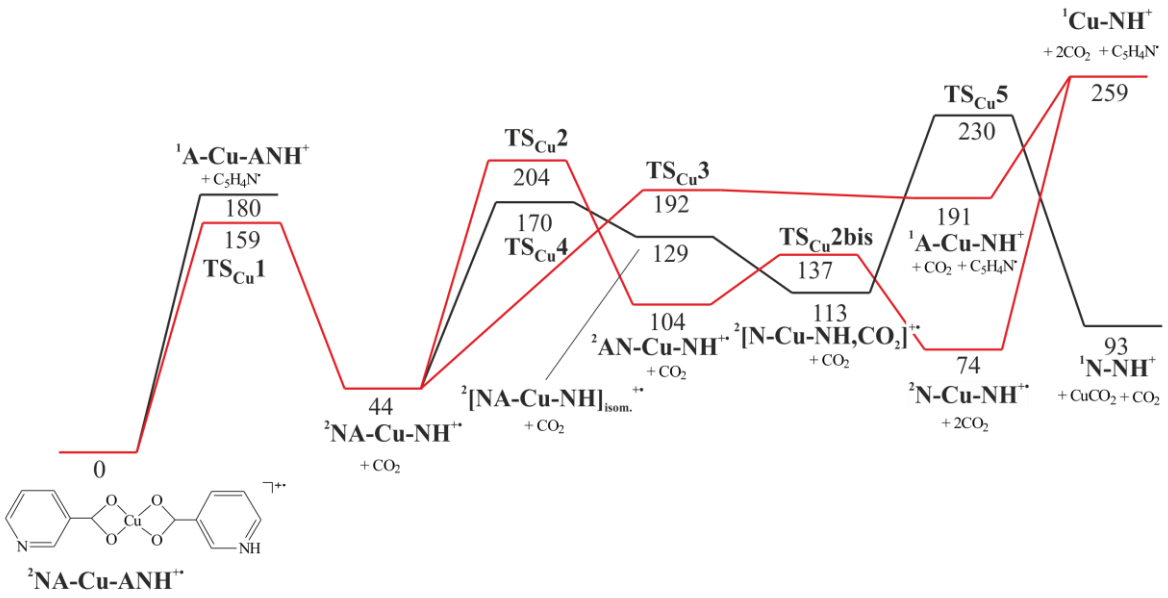

Figure 5. Potential energy diagram for the dissociation of ^{2}[Cu + 2NAH – H]$^{+\bullet}$ complex (relative energies in kJ mol^{-1}). Red lines represent the experimentally observed dissociation pathways and black lines the non-observed ones.

Now, starting from NA-Cu-NH$^{+\bullet}$, the 3-pyridinyl radical part of NA may be lost via **TS$_{Cu}$6** by direct dissociation of the C–C(O$_2$(Cu)) bond leading to a closed shell cationic species A-Cu-NH$^+$. However, the calculations indicate that the CO$_2$ moiety of A-Cu-NH$^+$ is rather weakly bonded (CO$_2$ loss requires 259 - 191 = 68 kJ mol^{-1}) having a OCO$^{\cdots}$Cu-NH$^+$ structure rather than (η^2-CO$_2$)-Cu-NH$^+$ - the latter would have contained the anticipated binding motif ***a*** of Scheme 1. For the ultimate dissociation product, Cu-ANH$^+$, the copper atom is formally Cu(I), meaning that the homolytic bond dissociation resulting from pyridinyl loss leads to electronic reduction of the metal. According to the calculations the alternative to pyridinyl loss from NA-Cu-NH$^{+\bullet}$ is loss of the second carboxylate group in the form of CO$_2$ requires slightly higher energy, in good agreement with the experimental observations. Out of several possible mechanisms for this second CO$_2$ loss, the one with the over-all lowest barrier corresponds first to a rearrangement of the NA-Cu-NH$^{+\bullet}$ ion leading to the AN-Cu-NH$^{+\bullet}$ ion via a 160 kJ mol^{-1} barrier (**TS$_{Cu}$2**) and then to the facile loss of the CO$_2$ moiety from this ion (through the transition structure **TS$_{Cu}$2bis**). Further dissociation of the doubly decarboxylated species N-Cu-NH$^{+\bullet}$ by 3-pyridyl radical loss to give Cu-NH$^+$ proceeds without barrier and is predicted to require 259 kJ mol^{-1}.

The direct loss of 3-pyridinyl radical from NA-Cu-ANH$^{+\bullet}$ to give A-Cu-ANH$^+$ was calculated to be without reverse critical energy, with products at 180 kJ mol^{-1}. The fact that the experiment only shows a minor peak resulting from this reaction indicates that the calculated value may be somewhat too low. Alternatively, further loss of CO$_2$ from A-Cu-ANH$^+$ to give Cu-ANH$^+$ in rather favourable (at 247 kJ mol^{-1}, not shown in the diagram). Also in A-Cu-ANH$^+$, the terminal CO$_2$ is weakly bonded, not possessing the sought-after (η^2-CO$_2$) moiety.

In conclusion, the computational data are consistent with the observed dissociation patterns showing kinetic rather than thermodynamic product control. Finally, we note that **TS$_{Cu}$5**

giving rise to $CuCO_2$ loss from NA-Cu-ANH$^{+\bullet}$ is expected to be energetically more favourable than forming Cu-NH$^+$. The latter is nevertheless showing a slightly higher signal than the former in the CID spectrum (*m/z* 142 vs *m/z* 157, Figure 3b) and becomes clearly higher on the SORI-CID spectrum. This observation is again consistent with kinetic control of the reaction favouring direct bond cleavage.

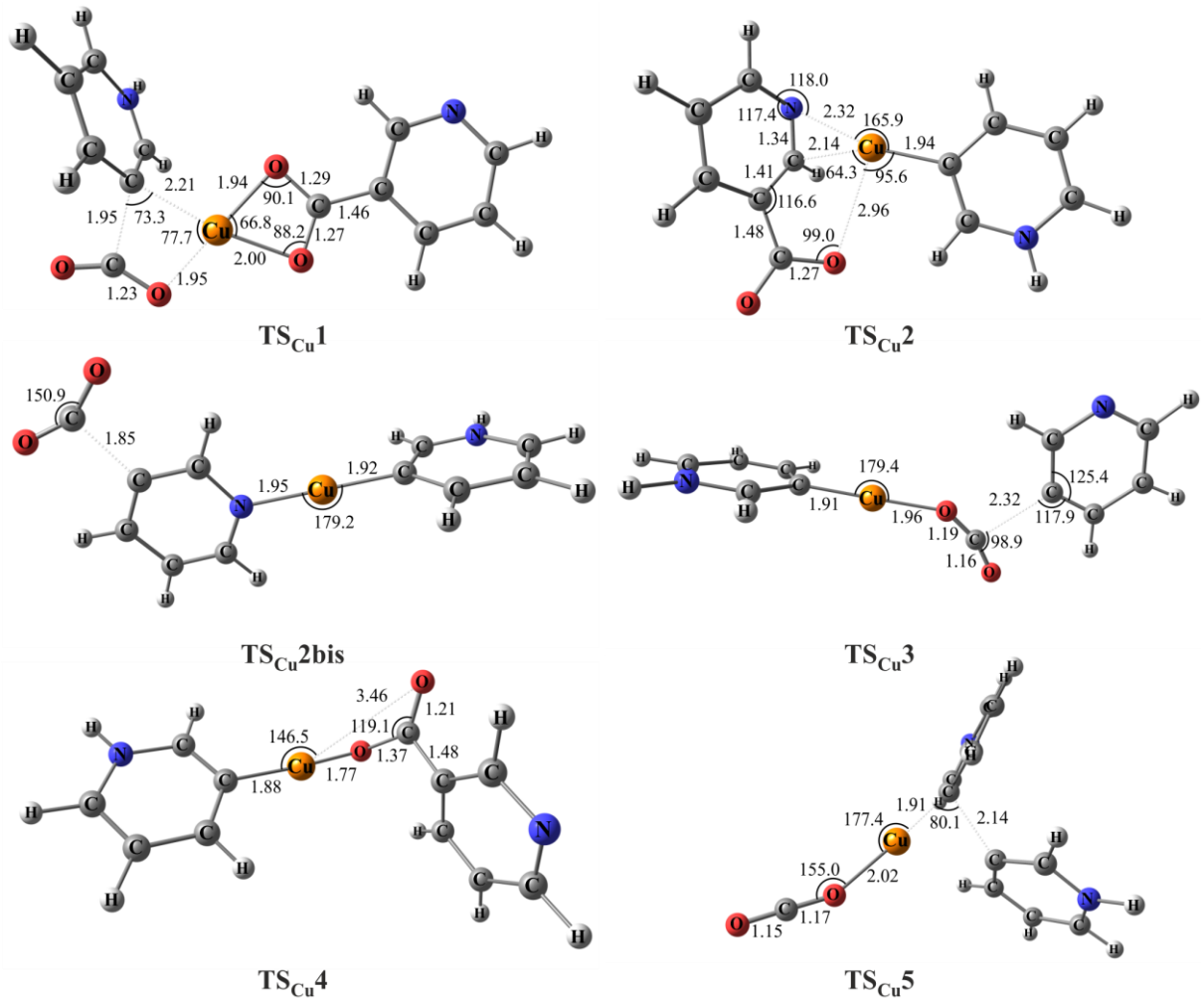

Figure 6. Geometry optimized transition structures involved in dissociation of ^{2}[Cu + 2NAH – H]$^{+\bullet}$ complex. Bond lengths are in Å and angles in degrees.

Figure 7 displays the potential energy diagram computed for the various dissociation pathways for [Ni + 2NAH – H]$^+$ for the triplet electronic state. The diagram describing the energetically slightly higher singlet state is shown in the Supplementary information. In analogy to the copper case described above, loss of CO_2 occurs via a C–C bond activation pathway via **TS$_{3Ni}$1** at 156 kJ mol^{-1}, giving the singly decarboxylated ion at 61 kJ mol^{-1}. Comparing Figures 5 and 7 shows that the energetic requirements are rather similar for the two cases. The same is apparently the case for the second CO_2 loss, however despite the quite similar energetic requirement, **TS$_{3Ni}$2** is completely different from **TS$_{Cu}$2**. In the former case (Figure 7) insertion of the nickel atom into the C–(CO_2) bond leads to a considerable elongation of that bond (bond length = 2.06 Å) leading directly to the fully dissociated

products, while in the latter case the process occurs in two steps: rearrangement to the N-coordinated NA-Cu-NH^+ to AN-Cu-NH^+ followed by CO_2 loss. Interestingly, N-Cu-NH^+ is 99 kJ mol^{-1} more stable than N-Ni-NH^+ in relative terms, reflecting the stronger binding of nitrogen ligands to Cu(II) compared to Ni(II), as also seen in the calculations of the dimeric parent complexes described above (Supplementary information).

The experimentally observed loss of $NiCO_2$ from the singly decarboxylated ion NA–Ni–NH^+ can be described as a two-steps reaction, first requiring transfer of the 3-pyridinyl moiety to the metal via $\mathbf{TS_{3Ni}4}$ leading to the ion-dipole complex [N-Ni-NH,CO_2]$^+$ followed by $NiCO_2$ loss via $\mathbf{TS_{3Ni}5}$ to the fully dissociated products at 132 kJ mol^{-1}. (Also displayed in Figure 7 is the path to formation of ^{1}N-NH^+ via the more energy demanding loss of nickel atom ($\mathbf{TS_{3Ni}3}$) starting from ^{3}N-Ni-NH^+ resulting as well in a formal loss of $NiCO_2$ from singly decarboxylated ion NA–Ni–NH^+.) The calculations predict that the $NiCO_2$ entity is not covalently bonded as in motif **a** (Scheme 1), but is essentially a complex between a nickel atom and CO_2. It is, however, noteworthy that in the singlet electronic state the energy minimum of $NiCO_2$ is predicted to be a side-on adduct in which the Ni atom binds to both C and one of the terminal O atoms. Interestingly, this dissociation is leading to the formation of a new C-C bond, namely the ^{1}N-NH^+ ion.

The fact that $\mathbf{TS_{3Ni}5}$ is computed to be 40 kJ mol^{-1} higher than $\mathbf{TS_{3Ni}2}$ could reflect the level of accuracy of the computational model since the abundances of the CID signals for the successive losses of two CO_2 molecules compared to CO_2 loss followed by $NiCO_2$ loss are similar. This observation could be also consistent with the fact that dissociation of this complex is driven by thermodynamic factors instead of kinetic ones, favouring thus formation of the most stable products. This would point out the large difference between copper and nickel complexes by means of dissociation behaviour although from a first sight both complexes seem to roughly behave similarly.

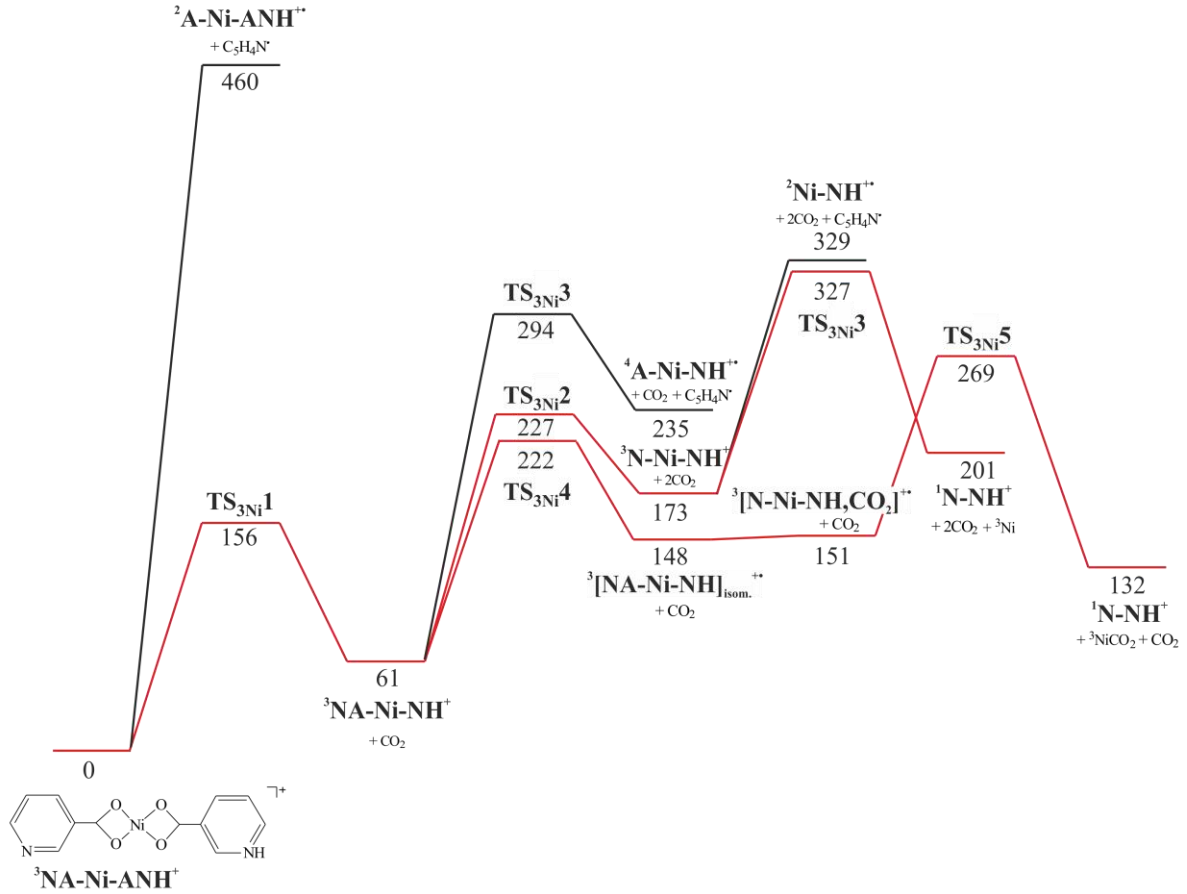

Figure 7. Potential energy diagram for the dissociation of the triplet [Ni + 2NAH – H]$^+$ complex (relative energies in kJ mol^{-1}). Red lines represent the experimentally-observed dissociation pathways and black lines the non-observed ones.

Again starting from the intermediate NA–Ni–NH$^+$, we performed calculations for the unobserved loss of the 3-pyridinyl radical for comparison with the copper system, for which it is observed. Perhaps not unexpected, this homolytic dissociation from the even electron nickel species display a transition state geometry **TS_{3Ni}6** at 294 kJ mol^{-1} in contrast to the open shell copper congener for which this only requires 192 kJ mol^{-1}. In line with this way of reasoning, we also note that the direct homolytic C–C cleavage from the parent NA–Ni–ANH$^+$ complex is predicted to require more than twice the amount of energy as the corresponding process in NA–Cu–ANH$^{+\bullet}$. Finally, as already mentioned, the relatively high-energy loss of CH_2O_2 would either be due to the successive H_2O and CO losses or loss of formic acid. The latter now seems more probable, based on result of our computational investigations as discussed in more detail in the Supplementary information.

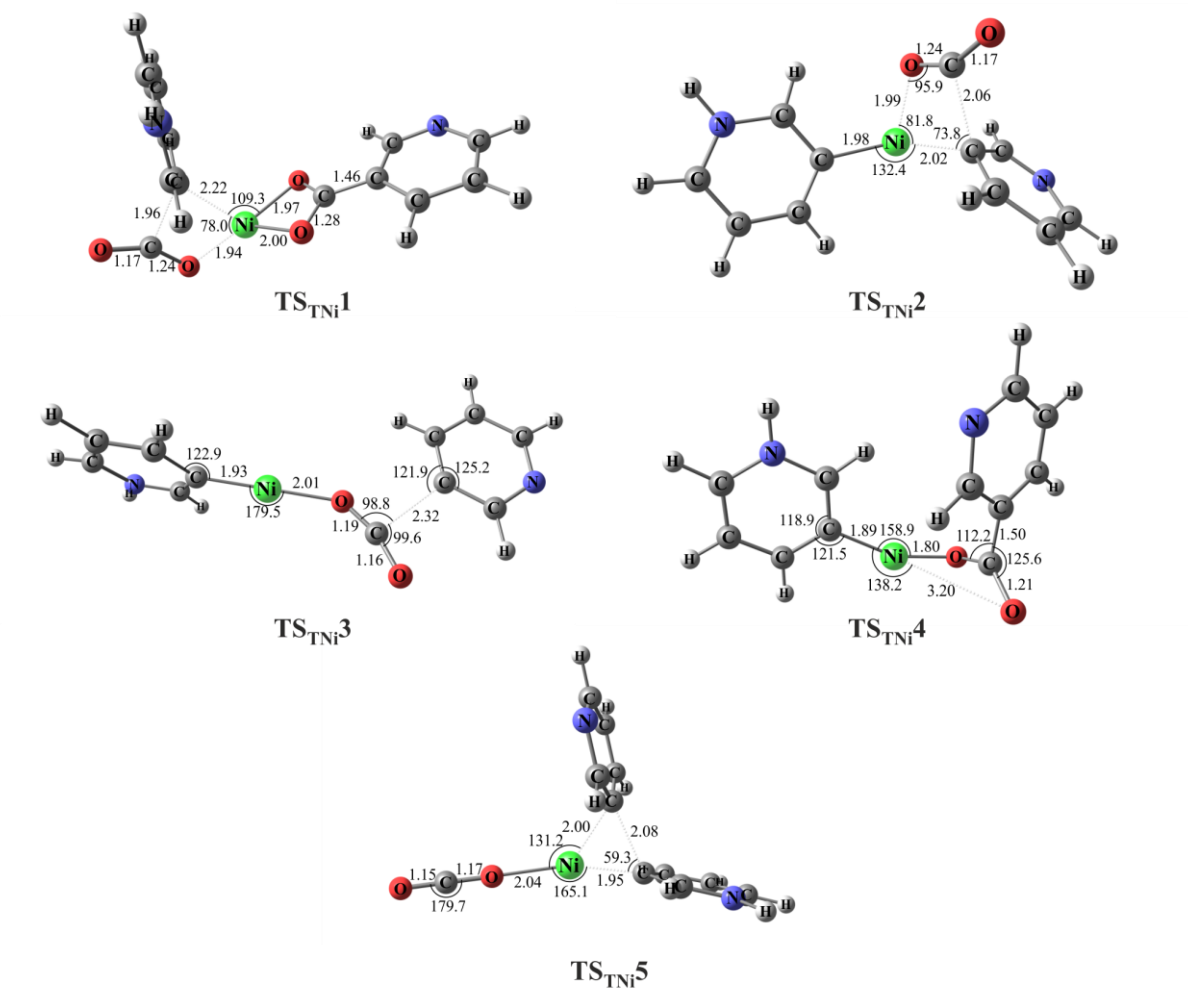

Figure 8. Geometry optimized transition structures involved in dissociation of triplet [Ni + 2NAH – H]$^+$ complex. Bond lengths are given in Å and angles in degree.

Discussion and conclusions

Previous mass spectrometric investigations [6-15] have demonstrated that ML(L–H)$^+$ complex ions formed between amino acids and Cu(II) and Ni(II) typically give CO_2 loss as the primary CID pathway. Following initial CO_2 loss, radical fragment loss was also known to be abundant but only for the odd electron copper species. The same applies to species where L = nicotinic acid, as demonstrated here, for which 3-pyridinyl loss is abundant from the decarboxylated complex NA-Cu-NH$^{+\bullet}$. We also see evidence for direct loss of 3-pyridinyl from the parent complex NA-Cu-ANH$^{+\bullet}$ but this is a minor reaction. In both cases it was of great interest to investigate the product ion structures, since they were considered to have a potential for containing the key M(η^2-O_2C) bonding motif. However, on the basis of our observations and in particular the quantum chemical calculations this type of structures seem to be of little relevance for cationic transition metals of this type, and carbon dioxide seems not to form particular strong bonds to copper in these cases. Instead of the oxidized state required for the simultaneous complexation of the two oxygen sites, copper prefers the reduced even electron Cu(I) state. Interestingly, the isoelectronic bare nickel atom behaves similarly, and seems not to give rise to a stable Ni(η^2-O_2C) geometry either. In this manner the electronically more flexible transition metal at least for the cationic species studied here,

behave very different from anionic alkali and alkali earth metals, which keep their oxidized form, thereby being able to accommodate bent CO_2 also when the C–C bond to the bond to the central carbon is broken.[1-4] In the future, it will be very interesting to study anionic forms of the same transition metals studied here and also zinc, to see how adding electrons will alter the structural and energetic landscapes.
One noteworthy reaction has nevertheless been observed and is characteristic for the Ni complex: the C-C bond formation leading to the $^{1}N\text{-}NH^{+}$ ion. Many catalytic cycles involve Nickel (II) complexes to form new C-C bonds. The last step of these cycles is usually an elimination of the metal leading to the new bond, which corresponds to the reaction observed (elimination of $NiCO_2$). We have investigated here the gas-phase mechanism of this reaction. This could be the first step of a work dedicated to probe a catalytic cycle involving Ni (II) and nicotinic acid.

We would also like to add a final note on the prospect of CO_2 uptake. Although $M(\eta^2\text{-}O_2C)$ species may be of relevance for the mechanism for CO_2 sequestration in various applications, it is of course possible to envisage reaction mechanisms not requiring this type of intermediates. In the present case, we may imagine the reverse of the observed decarboxylation reactions as prototypical CO_2 insertion reactions catalysed by a transition metal. However, in the absence of any stabilizing interactions, it seems clear that the transition states found would pose too high enthalpic and entropic requirements since the calculated energy barriers seem rather high in all cases encountered here.

Acknowledgments
This work was supported by the Norwegian Research Council by the Grant No. 179568/V30 to the Centre of Theoretical and Computational Chemistry through their Centre of Excellence program and the Norwegian Supercomputing Program (NOTUR) through a grant of computer time (Grant No. NN4654K). The TGE High field FT-ICR (CNRS) is gratefully acknowledged for the access to the FT-ICR mass spectrometer as well as Dr. E. Derat (IPCM) for providing us computational resources. CA acknowledges the European Regional Development Fund (ERDF) N°31708 and the région Haute Normandie for financial support. Finally, UPMC is also acknowledged for the financial support to permit one of the authors (E. U.) to come to Paris as a visiting professor.

References
[1] A.B. Attygalle, F.U. Axe, C.S. Weisbecker, Mild route to generate gaseous metal anions, Rapid Commun. Mass Spectrom., 25 (2011) 681-688.
[2] S. Curtis, J. DiMuzio, A. Mungham, J. Roy, D. Hassan, J. Renaud, P.M. Mayer, Reactions of Atomic Metal Anions in the Gas phase: Competition between Electron Transfer, Proton Abstraction and Bond Activation, J. Phys. Chem. A, 115 (2011) 14006-14012.
[3] S. Curtis, J. Renaud, J. Holmes, P. Mayer, Old acid, new chemistry. Negative metal anions generated from alkali metal oxalates and others, J. Am. Soc. Mass. Spectrom., 21 (2010) 1944-1946.

[4] H. Dossmann , C. Afonso, D. Lesage, J.-C. Tabet, E. Uggerud, Formation and Characterization of Gaseous Adducts of Carbon Dioxide to Magnesium, (CO2)MgX− (X=OH, Cl, Br), Angew. Chem. Int. Ed., 51 (2012) 6938-6941.
[5] A. Correa, R. Martín, Metal-Catalyzed Carboxylation of Organometallic Reagents with Carbon Dioxide, Angew. Chem. Int. Ed., 48 (2009) 6201-6204.
[6] S.R. Wilson, A. Yasmin, Y. Wu, Bipyridyl amino acid-metal complexes and their characterization by electrospray mass spectrometry, J. Org. Chem., 57 (1992) 6941-6945.
[7] C.L. Gatlin, F. Tureček, T. Vaisar, Gas-phase complexes of amino acids with Cu(II) and diimine ligands. Part I. Aliphatic and aromatic amino acids, J. Mass Spectrom., 30 (1995) 1605-1616.
[8] S. Bouchonnet, Y. Hoppilliard, G. Ohanessian, Formation and fragmentations of organometallic complexes involving aliphatic α-amino acids and transition metal cations—a plasma desorption mass spectrometry study, J. Mass Spectrom., 30 (1995) 172-179.
[9] F. Tureček, Copper-biomolecule complexes in the gas phase. The ternary way, Mass Spectrom. Rev., 26 (2007) 563-582.
[10] C. Afonso, A. Riu, Y. Xu, F. Fournier, J.-C. Tabet, Structural characterization of fatty acids cationized with copper by electrospray ionization mass spectrometry under low-energy collision-induced dissociation, J. Mass Spectrom., 40 (2005) 342-349.
[11] P. Wang, G. Ohanessian, C. Wesdemiotis, Cu(II)-catalyzed reactions in ternary [Cu(AA)(AA – H)]+ complexes (AA = Gly, Ala, Val, Leu, Ile, t-Leu, Phe), European Journal of Mass Spectrometry, 15 (2009) 325-335.
[12] C. Afonso, D. Lesage, F. Fournier, V. Mancel, J.-C. Tabet, Origin of enantioselective reduction of quaternary copper d,l amino acid complexes under vibrational activation conditions, Int. J. Mass spectrom., 312 (2012) 185-194.
[13] D. Zhang, W.A. Tao, R.G. Cooks, Chiral resolution of d- and l-amino acids by tandem mass spectrometry of Ni(II)-bound trimeric complexes, Int. J. Mass spectrom., 204 (2001) 159-169.
[14] R. Jirásko, M. Holčapek, L. Kolářová, M. Nádvorník, A. Popkov, Characterization of Ni(II) complexes of Schiff bases of amino acids and (S)-N-(2-benzoylphenyl)-1-benzylpyrrolidine-2-carboxamide using ion trap and QqTOF electrospray ionization tandem mass spectrometry, J. Mass Spectrom., 43 (2008) 1274-1284.
[15] A.R.M. Hyyryläinen, J.M.H. Pakarinen, F. Fülöp, P. Vainiotalo, Diastereochemical differentiation of some cyclic and bicyclic β-amino acids, via the kinetic method, J. Am. Soc. Mass. Spectrom., 20 (2009) 34-41.
[16] K. Giles, J.P. Williams, I. Campuzano, Enhancements in travelling wave ion mobility resolution. , Rapid Commun. Mass Spectrom., 25 (2011) 1559-1566.
[17] M.F. Mesleh, J.M. Hunter, A.A. Shvartsburg, G.C. Schatz, M.F. Jarrold, Structural Information from Ion Mobility Measurements: Effects of the Long-Range Potential, J. Phys. Chem. , 100 (1996) 16082-16086.
[18] A.A. Shvartsburg, M.F. Jarrold, An exact hard-spheres scattering model for the mobilities of polyatomic ions. , Chem. Phys. Lett., (1996) 86-91.
[19] S.C. Henderson, J. Li., A.E. Counterman, D.E. Clemmer, Intrinsic Size Parameters for Val. Ile. Leu. Gln. Thr. Phe. and Trp Residues from Ion Mobility Measurements of Polyamino Acid Ions., J. Phys. Chem. B 103 (1999) 8780-8785.
[20] M.J. Frisch, G.W. Trucks, H.B. Schlegel, G.E. Scuseria, M.A. Robb, J.R. Cheeseman, G. Scalmani, V. Barone, B. Mennucci, G.A. Petersson, H. Nakatsuji, M. Caricato, X. Li, H.P. Hratchian, A.F. Izmaylov, J. Bloino, G. Zheng, J.L. Sonnenberg, M. Hada, M. Ehara, K. Toyota, R. Fukuda, J. Hasegawa, M. Ishida, T. Nakajima, Y. Honda, O. Kitao, H. Nakai, T. Vreven, J.A. Montgomery, J.E. Peralta, F. Ogliaro, M. Bearpark, J.J. Heyd, E. Brothers, K.N. Kudin, V.N. Staroverov, R. Kobayashi, J. Normand, K. Raghavachari, A. Rendell, J.C.

Burant, S.S. Iyengar, J. Tomasi, M. Cossi, N. Rega, J.M. Millam, M. Klene, J.E. Knox, J.B. Cross, V. Bakken, C. Adamo, J. Jaramillo, R. Gomperts, R.E. Stratmann, O. Yazyev, A.J. Austin, R. Cammi, C. Pomelli, J.W. Ochterski, R.L. Martin, K. Morokuma, V.G. Zakrzewski, G.A. Voth, P. Salvador, J.J. Dannenberg, S. Dapprich, A.D. Daniels, Farkas, J.B. Foresman, J.V. Ortiz, J. Cioslowski, D.J. Fox, Gaussian 09, Revision B.01, in, Wallingford CT, 2009.
[21] M.Y. Combariza, R.W. Vachet, Effect of Coordination Geometry on the Gas-Phase Reactivity of Four-Coordinate Divalent Metal Ion Complexes, J. Phys. Chem. A, 108 (2004) 1757-1763.
[22] J.R. Hartman, R.W. Vachet, W. Pearson, R.J. Wheat, J.H. Callahan, A comparison of the gas, solution, and solid state coordination environments for the copper(II) complexes of a series of aminopyridine ligands of varying coordination number, Inorg. Chim. Acta, 343 (2003) 119-132.
[23] D.M. Black, A.H. Payne, G.L. Glish, Determination of Cooling Rates in a Quadrupole Ion Trap, J. Am. Soc. Mass Spectrom., 17 (2006) 932-938.
[24] S.A. McLuckey, D.E. Goeringer, Slow Heating Methods in Tandem Mass Spectrometry, J. Mass Spectrom., 32 (1997) 461-474.
[25] J. Laskin, M. Byrd, J. Futrell, Internal energy distributions resulting from sustained off-resonance excitation in FTMS. I. Fragmentation of the bromobenzene radical cation, Int. J. Mass Spectrom., 195/196 (2000) 285–302.

Supplementary information

Unimolecular dissociation characteristics of cationic complexes between nicotinic acid and Cu(II) and Ni(II).

Héloïse Dossmann,[a] Carlos Afonso,[a.b] Jean-Claude Tabet[a] and Einar Uggerud[c]

[a] Institut Parisien de Chimie Moléculaire, Université Pierre et Marie Curie-Paris 6, UMR 7201- FR2769, Place Jussieu, F-75252 Paris Cedex 05, France, [b] Université de Rouen, UMR CNRS 6014 COBRA, 1 rue Tesnière, 76130 Mont-Saint-Aignan, France and [c] Massespektrometrilaboratoriet og Senter for teoretisk og beregningsbasert kjemi (CTCC), Kjemisk institutt, Universitetet i Oslo, Postboks 1033 Blindern, N-0315 Oslo, Norway. E-mail: heloise.dossmann@upmc.fr or einar.uggerud@kjemi.uio.no

I- Theoretical method

To test the validity of the method and basis set used in this work (B3LYP/6-31G(d.p)). we have performed some comparison between calculated and experimental bond dissociation energies found in the literature for some copper and nickel complexes. Data and results are shown in Table S1. Agreement between experiment and theory is quite good: obtained standard deviations are 8 kJ/mol for copper and 14 kJ/mol for nickel complexes.

Table S1. Calculated enthalpies $H°_{total}$ (in hartrees, H) and bond dissociation energies (in kJ/mol) of selected copper and nickel complexes.

	$H°_{total}$ (H)[a]	Bond dissociation energies	
		Calculated[b]	Experimental
Cu^+	-1640.174546		
Ni^+	-1507.957103		
NH_3	-56.544587		
Pyrrole	-210.143394		
$Cu(NH_3)^+$	-1696.812257	244	237[c]
$Cu(NH_3)^{2+}$	-1753.442564	235	248[c]
$Cu(Pyrrole)^+$	-1850.410481	243	246[d]
$Cu(Pyrrole)^{2+}$	-2060.617313	205	213[d]
$Ni(NH_3)^+$	-1564.598346	254	238[c]
$Ni(NH_3)^{2+}$	-1621.223874	233	251[c]
$Ni(Pyrrole)^+$	-1718.197778	255	267.8[d]
$Ni(Pyrrole)^{2+}$	-1928.408831	217	222[d]

[a] Corresponds to the sum of electronic electronic and thermal enthalpies and is obtained at the B3LYP/6-31G(d.p) level of theory.
[b] Obtained at the B3LYP/6-31G(d.p) level of theory.
[c] Taken from D. Walter and P. B. Armentrout. J. Am. Chem. Soc.. **1998**. 120. 3176.
[d] Taken from A. Gapeev. C.-N. Yang. S. J. Klippenstein and R. C. Dunbar. J. Phys. Chem. A. **2000**. 104. 3246.

II- Results

1- Ion mobility experiments

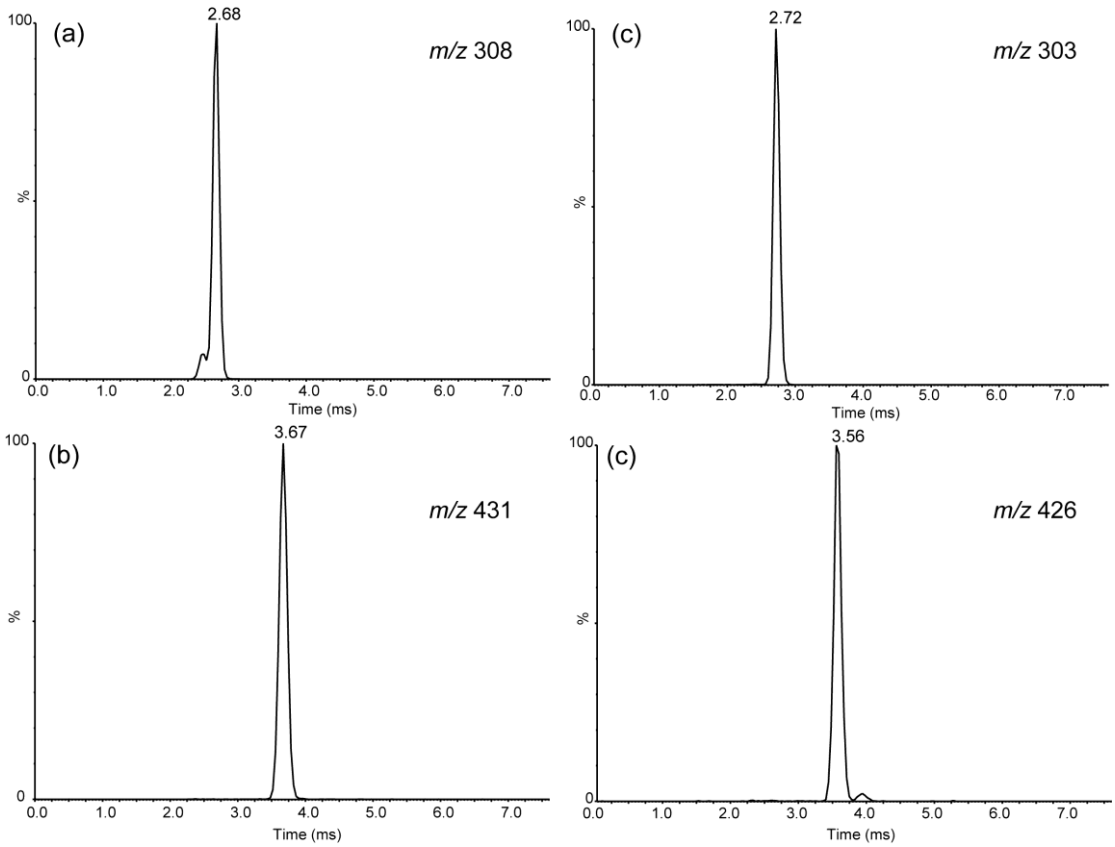

Figure S1. Ion mobility spectra of (a) $[2NAH - H + Cu]^{+\bullet}$ *m/z* 308, (b) $[3NAH - H + Cu]^{+\bullet}$ *m/z* 431, (c) $[2NAH - H + Ni]^{+}$ *m/z* 303 and (d) $[3NAH - H + Ni]^{+}$ *m/z* 426 recorded with a wave velocity of 600 m/s and wave height of 40 V.

Table S2. Experimental collision cross sections (CCS) (polyAla calibration) obtained for $[M + 2NAH - H]^{+}$ and $[M + 3NAH - H]^{+}$ complexes (M = Cu, Ni).

Ion	**Drift time (ms)**	**CCS (Å^2)**
$[2NAH - H + Cu]^{+\bullet}$	2.46	94.0
$[2NAH - H + Cu]^{+\bullet}$	2.68	100.3
$[3NAH - H + Cu]^{+\bullet}$	3.67	125.7
$[2NAH - H + Ni]^{+}$	2.72	101.4
$[3NAH - H + Ni]^{+}$	3.56	122.9
$[3NA - H + Ni]^{+}$	3.94	132.7

Table S3. Theoretical CCS determination of the most stable calculated forms of each $[M + 2NAH - H]^{+}$ complex (M = Cu, Ni).

Ion	Projection approximation (PA) (Å^2)	Exact hard sphere scattering (EHSS) (Å^2)	Trajectory method (TM) (Å^2)
^{2}**NA-Cu-ANH**$^{+\bullet}$	104.3	107.8	102.1
^{2}**NA-Cu-NAH**$^{+\bullet}$	104.3	108.1	102.2
^{2}**AN-Cu-NAH**$^{+\bullet}$	106.8	111.9	105.6
^{2}**NA-Cu-AHN**$^{+\bullet}$	103.3	106.9	101.7
^{2}**AN-Cu-ANH**$^{+\bullet}$	107.1	111.4	106.7
^{3}**NA-Ni-ANH**$^{+}$	104.2	107.7	102.3
^{3}**NA-Ni-AHN**$^{+}$	107.8	112.8	105.9
^{3}**AN-Ni-NAH**$^{+}$	107.1	112.4	106.3
^{1}**NA-Ni-ANH**$^{+}$	103.1	106.5	101.0
^{1}**NA-Ni-NAH**$^{+}$	103.2	106.9	101.5
^{1}**NA-Ni-AHN**$^{+}$	102.6	106.1	101.1

2- [M + 2NAH – H]$^+$ isomers (M = Cu, Ni)

For each [M + 2NAH – H]$^+$ complex studied (M = Cu, Ni), many structures have been tested. Optimized geometries of isomers having the lowest energy are presented in Figure S2 for copper complexes and in Figure S3 for nickel complexes. Total electronic energies and zero-point vibrational energies are given in Table S4.

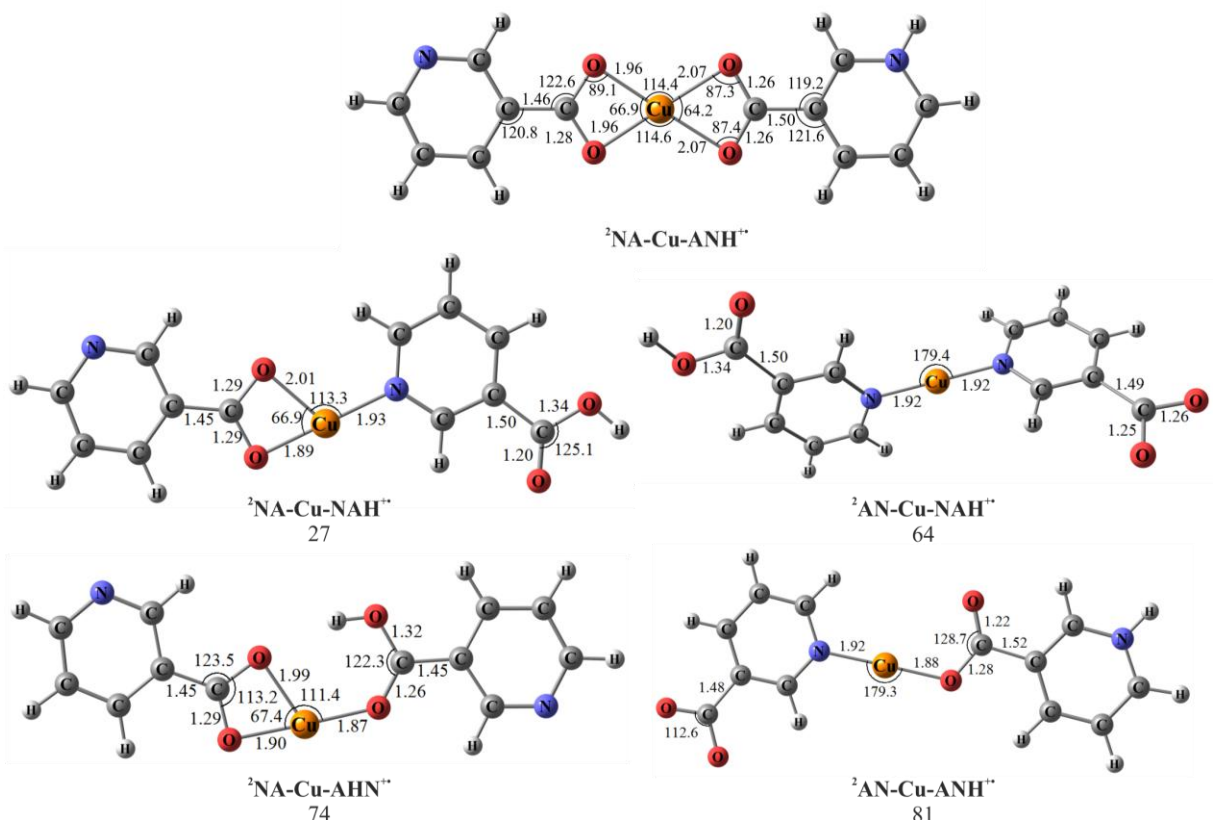

Figure S2. Geometry optimized structures and relative energies of the various [Cu + 2NAH – H]$^{+\bullet}$ complexes considered. Relative energies are in kJ/mol. bond lengths in Å and angles in degrees.

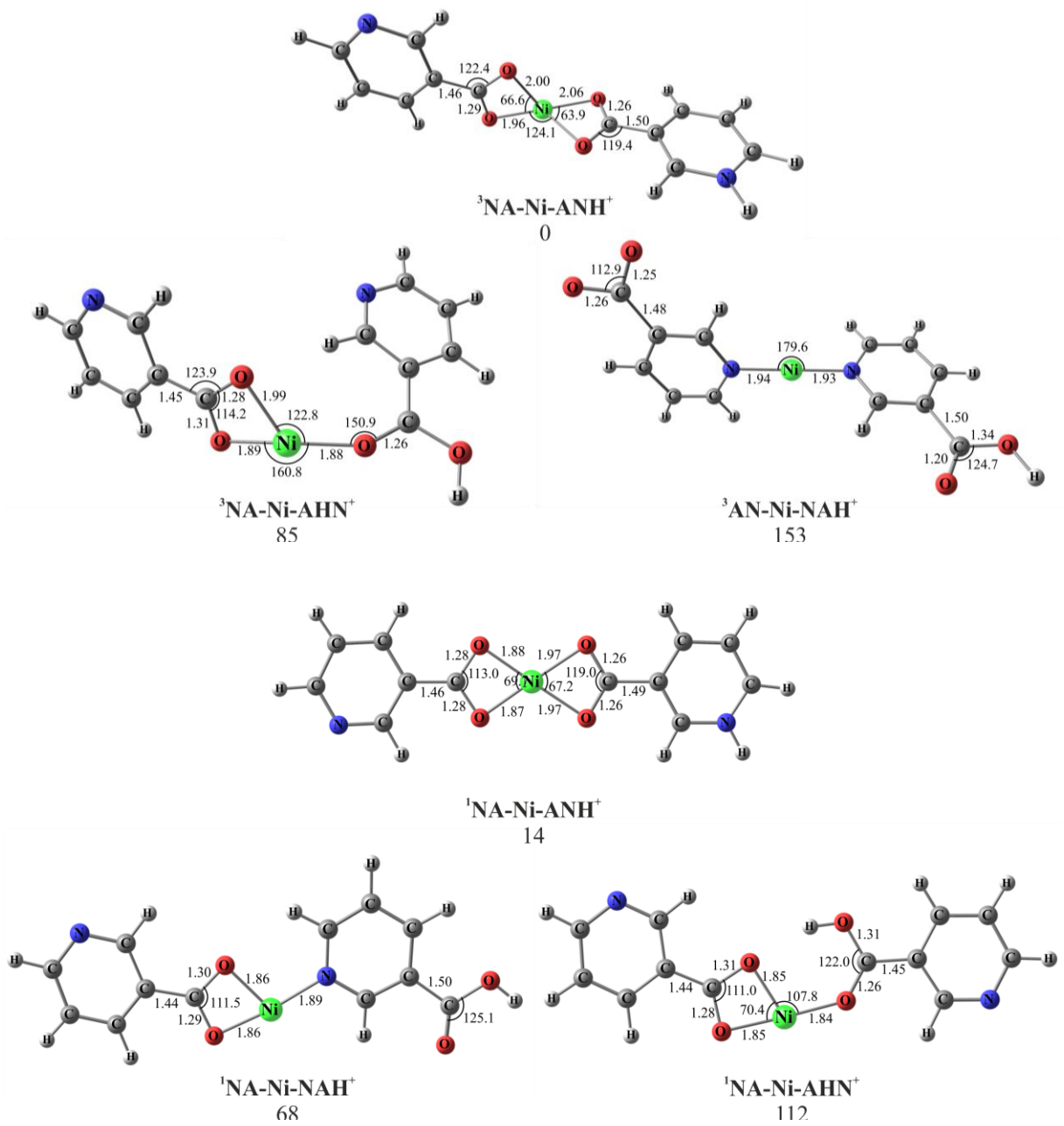

Figure S3. Geometry optimized structures and relative energies of the various $[Ni + 2NAH - H]^+$ complexes considered (singlet and triplet multiplicities). Relative energies are in kJ/mol, bond lengths in Å and angles in degrees.

3- <u>Dissociation of singlet $[Ni + 2NAH - H]^+$ complex</u>

As singlet dimeric form of $[Ni + 2NAH - H]^+$ is only 14 kJ/mol above the corresponding triplet, we have also considered dissociation of this ions. Results are presented on Figure S4.

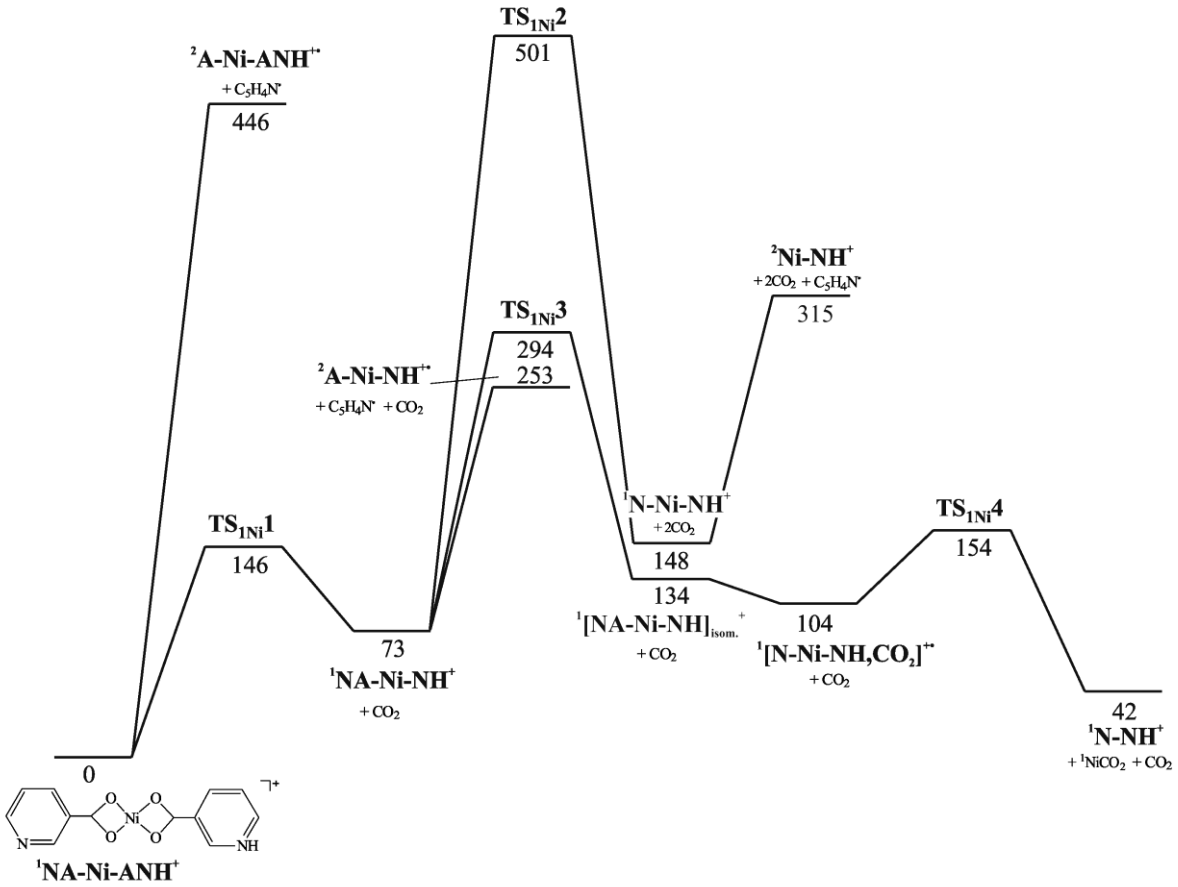

Figure S4. Complete potential energy diagram for the dissociation of singlet $[Ni + 2NAH - H]^+$ complex (relative energies in kJ/mol).

4- <u>HOCOH loss for NA-M-NH$^+$ ions (M = Cu, Ni)</u>

As outlined in the paper, activation of NA-Ni-NH$^+$ ion (*m/z* 259) shows a small signal corresponding to loss of H_2CO_2. This pathway seems to require a lot of energy as the fragment ion is only observed on the SORI-CID spectrum (FT-ICR) and not on the CID spectrum (ion trap). We have probed the fragmentation mechanism with theory. To this end, three losses have been tested: loss of CO_2/H_2, loss of CO/H_2O and loss of HOCOH. The latter shows the lowest energy requirement and is presented on Figures S5, S6 and S7 for Cu, triplet Ni and singlet Ni ions, respectively. Scheme S1 presents the different structures involved in this dissociation pathway.

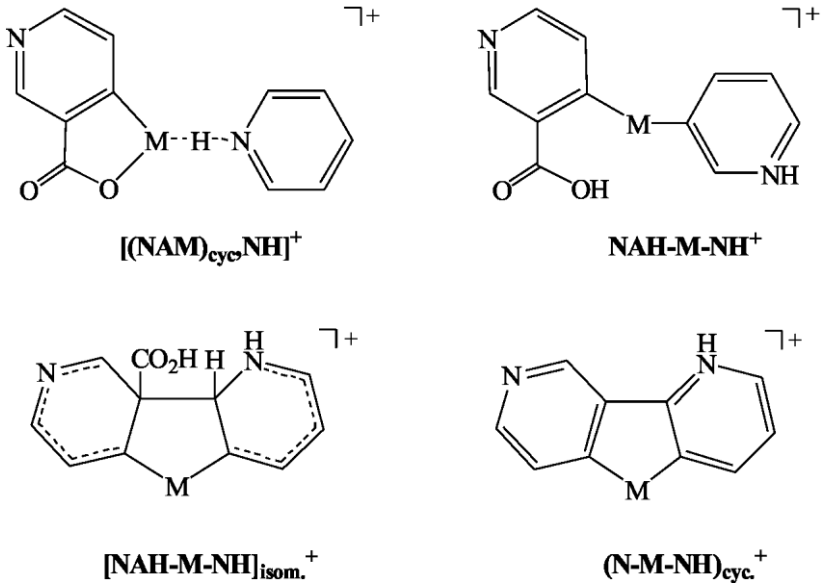

Scheme S1.

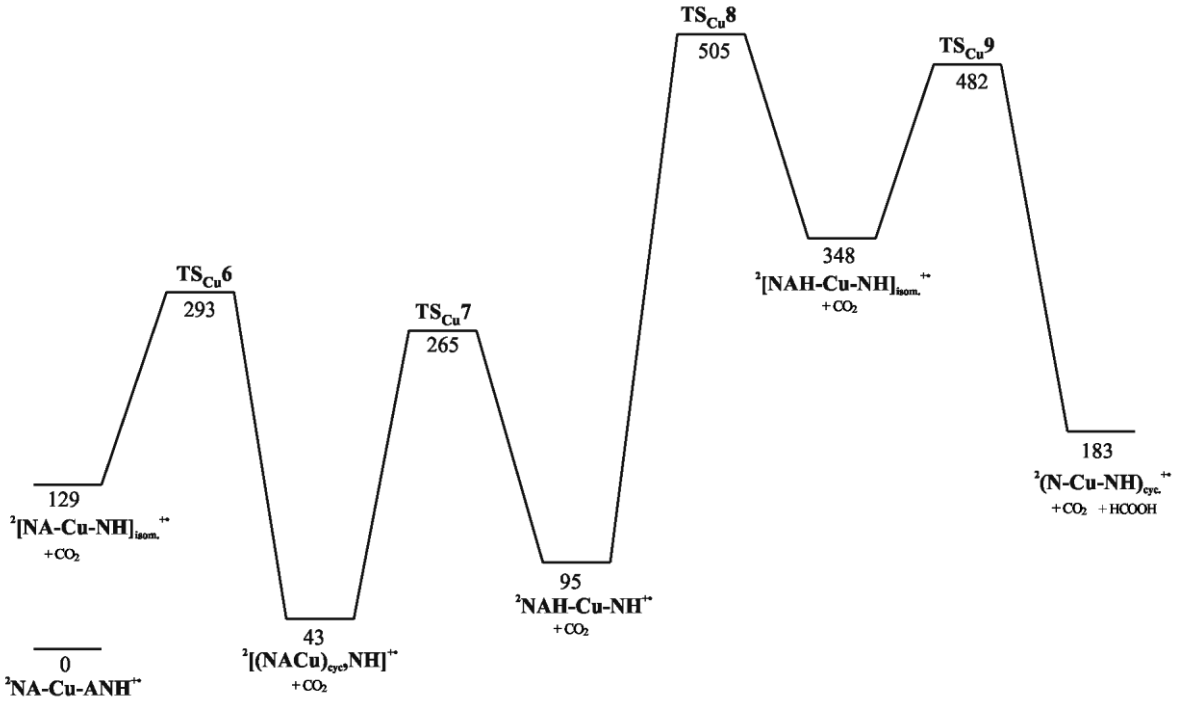

Figure S5. Potential energy diagram for HOCOH loss of NA-Cu-$NH^{+\bullet}$ ion (relative energies in kJ/mol).

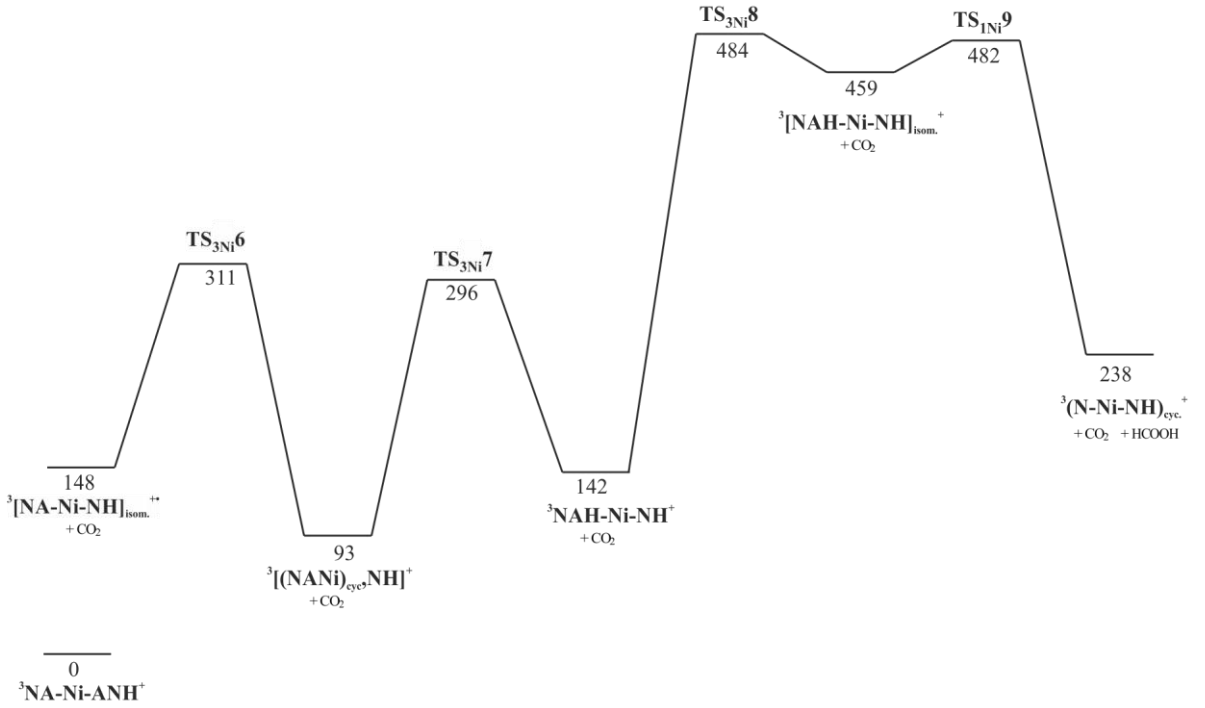

Figure S6. Potential energy diagram for HOCOH loss of triplet NA-Ni-NH$^+$ ion (relative energies in kJ/mol).

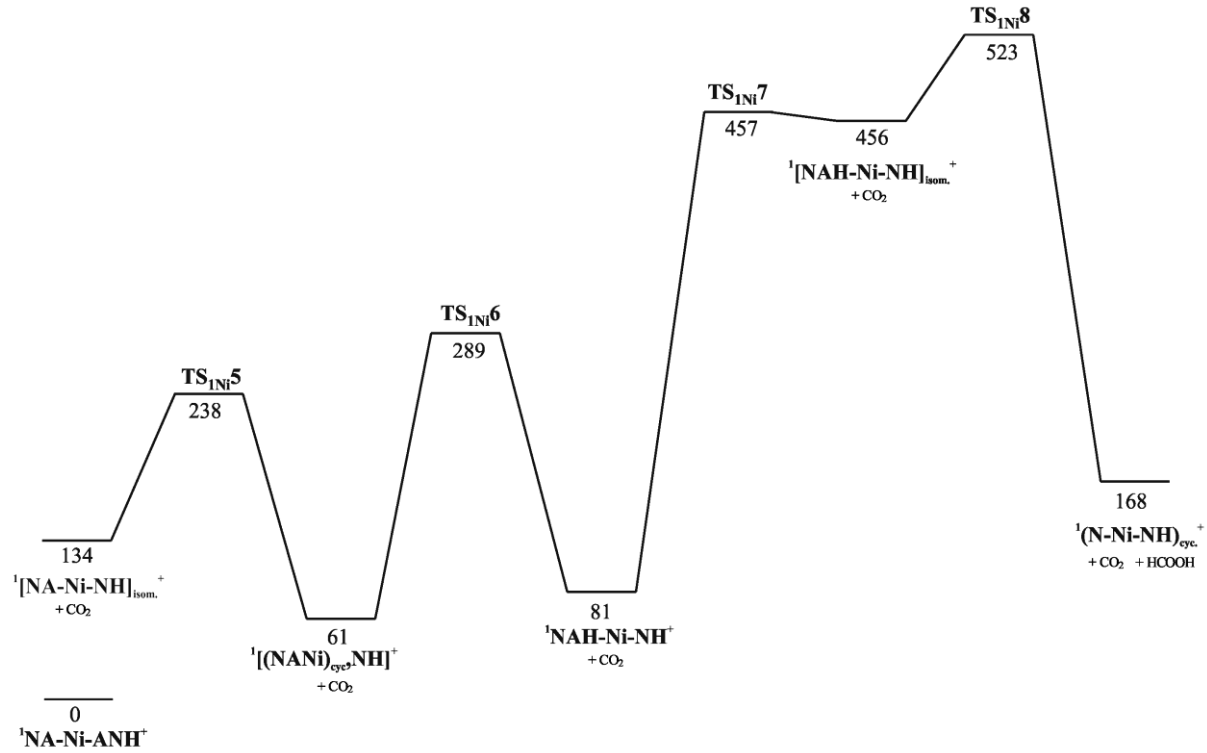

Figure S7. Potential energy diagram for HOCOH loss of singlet NA-Ni-NH$^+$ ion (relative energies in kJ/mol).

5- Total electronic energies

Table S4. Calculated electronic and zero-point energies (in hartrees, H) and relative energies (in kJ/mol) of all compounds studied in this work.

	Electronic energy (H)	Zero-point energy (H)	Relative energies (kJ/mol)[a]
$C_5H_4N^{\bullet}$	-247.6616314	0.075353	
$CuCO_2$	-1829.119215	0.0117684	
$^3NiCO_2$	-1696.897487	0.0117684	
$^1NiCO_2$	-1696.895855	0.0116117	
CO_2	-188.6469147	0.0116852	
HOCOH	-189.8277116	0.0337044	
$^1N\text{-}NH^+$	-495.8720078	0.1711818	
$^2NA\text{-}Cu\text{-}ANH^{+\bullet}$	-2513.678229	0.1991332	0
$^2NA\text{-}Cu\text{-}NAH^{+\bullet}$	-2513.666759	0.1980613	27
$^2AN\text{-}Cu\text{-}NAH^{+\bullet}$	-2513.651609	0.1967739	64
$^2NA\text{-}Cu\text{-}AHN^{+\bullet}$	-2513.648159	0.1973146	74
$^2AN\text{-}Cu\text{-}ANH^{+\bullet}$	-2513.64527	0.1971636	81
$^1A\text{-}Cu\text{-}ANH^+$	-2265.942809	0.1184316	180
$^2NA\text{-}Cu\text{-}NH^{+\bullet}$	-2325.011361	0.1844303	44
$^2[NA\text{-}Cu\text{-}NH]_{isom.}{}^{+\bullet}$	-2324.978193	0.183323	129
$^2AN\text{-}Cu\text{-}NH^{+\bullet}$	-2324.986905	0.1827894	104
$^2[N\text{-}Cu\text{-}NH.CO_2]^{+\bullet}$	-2324.981249	0.1805081	113
$^1A\text{-}Cu\text{-}NH^+$	-2077.288535	0.1041688	191
$^2N\text{-}Cu\text{-}NH^{+\bullet}$	-2136.349368	0.1689763	74
$^1Cu\text{-}NH^+$	-1888.615202	0.0914476	259
$^2[(NACu)_{cyc.}.NH]^{+\bullet}$	-2325.010001	0.1826306	43
$^2NAH\text{-}Cu\text{-}NH^{+\bullet}$	-2324.991337	0.1835604	95
$^2[NAH\text{-}Cu\text{-}NH]_{isom.}{}^{+\bullet}$	-2324.893579	0.1824399	348
$^2(N\text{-}Cu\text{-}NH)_{cyc.}{}^{+\bullet}$	-2135.1275932	0.1475816	183
$TS_{Cu}1$	-2513.614653	0.1962098	159
$TS_{Cu}2$	-2324.947608	0.1810283	204
$TS_{Cu}2bis$	-2324.972215	0.1805139	137
$TS_{Cu}3$	-2324.950363	0.1795035	192
$TS_{Cu}4$	-2324.9589594	0.1799813	170
$TS_{Cu}5$	-2324.935179	0.1790883	230
$TS_{Cu}6$	-2324.909777	0.177416	293
$TS_{Cu}7$	-2324.92016	0.177103	265
$TS_{Cu}8$	-2324.83004	0.1786082	505
$TS_{Cu}9$	-2324.8339511	0.1736697	482
$^3NA\text{-}Ni\text{-}ANH^+$	-2381.497359	0.1990403	0
$^3NA\text{-}Ni\text{-}AHN^+$	-2381.463429	0.1973178	85
$^3AN\text{-}Ni\text{-}NAH^+$	-2381.436601	0.1966705	153
$^2A\text{-}Ni\text{-}ANH^{+\bullet}$	-2133.645833	0.1186645	460
$^3NA\text{-}Ni\text{-}NH^+$	-2192.824225	0.1842097	61
$^3[NA\text{-}Ni\text{-}NH]_{isom.}{}^+$	-2192.790325	0.1837693	148
$^3[N\text{-}Ni\text{-}NH.CO_2]^+$	-2192.786627	0.1811459	151
$^4A\text{-}Ni\text{-}NH^{+\bullet}$	-1944.988004	0.01032565	235
$^3N\text{-}Ni\text{-}NH^+$	-2004.129857	0.1686841	173
$^3Ni\text{-}NH^{+\bullet}$	-1756.397944	0.0912691	329
$^3[(NANi)_{cyc.}.NH]^+$	-2192.810849	0.1831206	93
$^3NAH\text{-}Ni\text{-}NH^+$	-2192.792794	0.1836514	142

^{3}**[NAH-Ni-NH]$_{isom.}^{+}$**	-2192.6691323	0.1809934	459
^{3}**(N-Ni-NH)$_{cyc.}^{+}$**	-2002.9263087	0.1477897	238
TS$_{3Ni}$1	-2381.435175	0.1962401	156
TS$_{3Ni}$2	-2192.757475	0.1809301	227
TS$_{3Ni}$3	-2192.730081	0.1790621	294
TS$_{3Ni}$4	-2192.7601648	0.1814758	222
TS$_{3Ni}$5	-2192.739816	0.1792297	269
TS$_{3Ni}$6	-2192.7228702	0.1781693	311
TS$_{3Ni}$7	-2192.7282171	0.1779702	296
TS$_{3Ni}$8	-2192.6587624	0.1798774	484
TS$_{3Ni}$9	-2192.6536862	0.174121	482
^{1}**NA-Ni-ANH^{+}**	-2381.493265	0.2003651	0
^{1}**NA-Ni-NAH^{+}**	-2381.471283	0.1988613	54
^{1}**AN-Ni-AHN^{+}**	-2381.453929	0.1982462	98
^{2}**A-Ni-ANH$^{+\bullet}$**	-2133.645833	0.1186645	446
^{1}**NA-Ni-NH^{+}**	-2192.814973	0.1850423	73
^{1}**[NA-Ni-NH]$_{isom.}^{+}$**	-2192.790325	0.1837691	134
^{1}**[N-Ni-NH.CO$_2$]$^{+}$**	-2192.800513	0.1823189	104
^{2}**A-Ni-NH$^{+\bullet}$**	-1945.06924	0.1039974	253
^{1}**N-Ni-NH^{+}**	-2004.135434	0.1693794	148
^{1}**Ni-NH$^{+\bullet}$**	-1756.397944	0.0912691	315
^{1}**[(NANi)$_{cyc.}$.NH]$^{+}$**	-2192.81834	0.1838075	61
^{1}**NAH-Ni-NH^{+}**	-2192.811212	0.1845157	81
^{1}**[NAH-Ni-NH]$_{isom.}^{+}$**	-2192.66571	0.1822676	456
^{1}**(N-Ni-NH)$_{cyc.}^{+}$**	-2002.9482336	0.1486934	168
TS$_{1Ni}$1	-2381.434701	0.1975426	146
TS$_{1Ni}$2	-2192.645651	0.178966	501
TS$_{1Ni}$3	-2192.7269427	0.1813406	293
TS$_{1Ni}$4	-2192.7803906	0.1813129	154
TS$_{1Ni}$5	-2192.7459453	0.1790474	238
TS$_{1Ni}$6	-2192.726297	0.1785272	289
TS$_{1Ni}$7	-2192.665121	0.1811487	457
TS$_{1Ni}$8	-2192.6374416	0.1790051	523

[a] Energies are given relatively to the corresponding NA-M-NAH^{+} dimer (M = Cu, ^{3}Ni or ^{1}Ni).

6- Optimized geometries

Table S5. Cartesian coordinates (x,y,z) of optimized geometries of compounds studied in this work.

	x	y	y
$C_5H_4N^{\bullet}$			
C	1.273232	-0.6035	-0.000189
C	0.130658	-1.37343	-0.000068
C	-1.141235	-0.855898	0.000119
C	-1.234708	0.541062	0.000179
C	-0.051614	1.280372	0.000055
N	1.168474	0.738053	-0.000123
H	-2.027066	-1.482057	0.00021
H	2.273896	-1.021146	-0.000339
H	-2.198135	1.039197	0.000318
H	-0.086012	2.365999	0.0001
$CuCO_2$			
C	0	-2.623497	0
O	-1.160819	-2.623972	0
O	1.160819	-2.624093	0
Cu	0	1.990535	0
$TNiCO_2$			
C	-2.470352	0.091945	0
O	-1.442198	0.632662	0
O	-3.496451	-0.449562	0
Ni	1.940404	-0.072017	0
$NiCO_2$			
C	0.974269	0.048075	0.000002
O	2.010902	-0.522161	-0.000026
O	0.371445	1.147803	0.000051
Ni	-0.889442	-0.189056	-0.000008
CO_2			
C	0	0	0
O	0	0	1.160915
O	0	0	-1.160915
HOCOH			

C	0	0.421673	0
O	1.159534	0.11739	0
O	-1.028735	-0.446678	0
H	-0.66123	-1.345217	0
H	-0.385164	1.449485	0
^{1}N-NH^{+}			
C	-1.496922	-1.103113	-0.412243
C	-0.78814	0.034782	0.006205
C	-1.533094	1.152345	0.408228
C	-2.917768	1.076709	0.388624
C	-3.517555	-0.112739	-0.029769
H	-0.967318	-1.978882	-0.781159
H	-1.041898	2.053596	0.758712
H	-3.526325	1.914985	0.703728
H	-4.598167	-0.211496	-0.043528
C	0.686016	0.045658	0.00299
C	1.436548	1.172795	-0.382771
C	1.40586	-1.084656	0.385924
C	2.828212	1.150139	-0.383642
H	0.91926	2.069366	-0.703314
H	0.938079	-1.997212	0.729049
C	3.487965	-0.004636	-0.008351
H	3.402075	2.016081	-0.685938
H	3.242762	-1.918522	0.647168
H	4.563384	-0.11358	0.012308
N	-2.822822	-1.181639	-0.429704
N	2.754453	-1.075224	0.359961
^{1}A-Cu-ANH^{+}			
C	-4.857931	0.20217	0.000949
O	-3.783831	-0.266086	0.000606
O	-5.91651	0.644017	0.001345
C	2.751864	-1.064455	0.000267
C	2.202857	0.205901	-0.000089
C	3.062964	1.307206	-0.000005
C	4.44668	1.121527	0.000437
C	4.95163	-0.162464	0.000787
N	4.094034	-1.208555	0.00069
H	2.623274	2.298368	-0.000287
H	2.143891	-1.958729	0.000225
H	5.128927	1.961193	0.000513
H	6.007162	-0.397782	0.00114
C	0.694811	0.404889	-0.000539
O	0.255424	1.544026	-0.000856
O	0.030036	-0.701288	-0.000485
H	4.478401	-2.14841	0.000946
Cu	-1.835796	-0.453406	-0.000796
^{2}NA-Cu-NH^{+}			
C	3.24112	1.382619	-0.000376
C	2.822463	0.043543	-0.000014
C	3.791367	-0.968674	0.000313
C	5.125895	-0.595449	0.000259
C	5.4374	0.766769	-0.000114
N	4.520584	1.742252	-0.000428
H	3.49238	-2.009706	0.000599
H	2.507791	2.182736	-0.000623
H	5.915624	-1.336084	0.000504
H	6.473594	1.090955	-0.000162
C	1.401978	-0.288063	0.000047
O	0.97694	-1.49978	0.000523
O	0.480846	0.607469	-0.000201
C	-2.804891	1.164832	0.000564
C	-2.660716	-0.217735	0.000092
C	-3.853871	-0.961672	-0.000401
C	-5.108642	-0.343783	-0.000451
C	-5.178652	1.033564	-0.000001
N	-4.02976	1.742178	0.00049
H	-3.821181	-2.046217	-0.000768
H	-1.965529	1.849928	0.00102
H	-6.022976	-0.922795	-0.000837
H	-6.102844	1.595127	-0.000009
H	-4.086905	2.756202	0.000837
Cu	-0.854093	-0.914082	-0.000106
^{2}[NA-Cu-NH]$_{isom.}^{+\bullet}$			
C	-1.414025	0.712395	-0.873302
C	-2.405786	0.120485	-0.060986
C	-3.117534	0.9464	0.818704
C	-2.778687	2.286552	0.873666
C	-1.717615	2.761776	0.076144
N	-1.051323	2.002407	-0.78746
H	-3.908764	0.526803	1.428786
H	-1.005264	0.160416	-1.723698
H	-3.301277	2.969453	1.532483
H	-1.410725	3.800853	0.142736
C	-2.611913	-1.369808	-0.112728
O	-3.695193	-1.895362	-0.081432
O	-1.456628	-2.009431	-0.15679
C	2.973182	-1.092099	0.480876
C	1.902948	-0.326463	0.029836
C	2.224471	0.984808	-0.377267
C	3.531827	1.477102	-0.331782
C	4.543322	0.659301	0.127083
N	4.233942	-0.59384	0.518349
H	1.437988	1.641393	-0.738448
H	2.884652	-2.115275	0.825193
H	3.76632	2.484538	-0.650297
H	5.581559	0.953962	0.196626
H	4.981044	-1.193582	0.854968
Cu	0.107916	-1.062513	-0.068285
^{2}AN-Cu-NH^{+}			
C	1.968746	-0.321667	0.00195
C	3.343792	-0.11054	0.004471
C	3.836667	1.194323	-0.021633
C	2.925928	2.243847	-0.050111
C	1.568013	1.955669	-0.051313
N	1.086727	0.693182	-0.025732
H	4.905689	1.374634	-0.019609
H	1.567845	-1.32792	0.023067
H	3.255494	3.274399	-0.070982
H	0.832238	2.749964	-0.072969
C	4.260663	-1.276299	0.034725
O	5.513117	-1.172566	0.044257
O	3.874581	-2.469632	0.052834
C	-3.452692	-0.268141	-1.140682
C	-2.716082	-0.02649	0.018201
C	-3.472857	-0.08305	1.210743
C	-4.843283	-0.357283	1.2284
C	-5.497445	-0.585459	0.036161
N	-4.783289	-0.533563	-1.106797
H	-2.983831	0.091127	2.163086
H	-3.025747	-0.262723	-2.135571
H	-5.400708	-0.395405	2.15544
H	-6.552419	-0.805785	-0.050407
H	-5.26488	-0.70242	-1.984023
Cu	-0.830622	0.339135	-0.016639
^{2}[N-Cu-NH.CO_2]$^{+\bullet}$			
C	1.727672	-1.417903	1.234251
C	1.253461	-0.877043	0.039637
C	1.782879	-1.337008	-1.171858
C	3.22883	-2.747415	-0.069333
H	1.440353	-0.967382	-2.133755
H	1.325329	-1.115027	2.196039
H	4.009366	-3.497225	-0.158607

C	2.150582	3.17919	-0.03616
O	1.138619	2.588997	0.000963
O	3.138691	3.765214	-0.071549
C	-2.97063	1.093308	0.131188
C	-1.9138	0.170659	0.010328
C	-2.294271	-1.159268	-0.129974
C	-4.614323	-0.640635	-0.033535
H	-1.588318	-1.973848	-0.231233
H	-2.758671	2.151441	0.244163
H	-3.825985	-2.507307	-0.256461
H	-5.619338	-1.038655	-0.061399
H	-5.115469	1.416307	0.204741
Cu	-0.004215	0.6315	0.02056
N	2.759836	-2.250507	-1.213774
C	2.753997	-2.3615	1.183897
H	3.163669	-2.795227	2.088714
N	-3.599922	-1.523246	-0.149031
C	-4.31216	0.696948	0.110874
^{1}A-Cu-NH^{+}			
C	3.960518	-0.002975	-0.00502
O	2.789138	-0.009453	-0.003362
O	5.107446	0.002585	-0.007552
C	-1.864239	-1.150121	0.0005
C	-1.109806	0.021237	0.002691
C	-1.868108	1.21265	0.000444
C	-3.265474	1.216519	-0.003813
C	-3.940448	0.013897	-0.005855
N	-3.220661	-1.126602	-0.003621
H	-1.36231	2.171755	0.002011
H	-1.434546	-2.143505	0.001887
H	-3.827657	2.141378	-0.005521
H	-5.017434	-0.082279	-0.009131
H	-3.71874	-2.01114	-0.005079
Cu	0.801999	-0.000079	0.006717
^{2}N-Cu-NH$^{+\bullet}$			
C	2.692197	-0.450863	-1.138893
C	4.061504	-0.44244	-1.125409
C	4.828887	-0.024466	-0.067863
C	4.117018	0.415263	1.054435
C	2.727699	0.399967	1.024027
N	2.015608	-0.021211	-0.041774
H	5.912929	-0.029207	-0.087445
H	2.109029	-0.785237	-1.98733
H	4.632332	0.765531	1.940573
H	2.155906	0.735905	1.880051
C	-2.61214	-1.086259	0.369012
C	-1.850483	0.020238	-0.005092
C	-2.612996	1.152858	-0.371384
C	-4.010646	1.164352	-0.359907
C	-4.688163	0.026212	0.02359
N	-3.969225	-1.059625	0.37476
H	-2.106205	2.061581	-0.677797
H	-2.184876	-2.032185	0.677029
H	-4.571619	2.045058	-0.645067
H	-5.76512	-0.060551	0.063611
H	-4.467919	-1.897265	0.656669
Cu	0.070469	-0.009895	-0.019527
^{1}Cu-NH^{+}			
C	-0.638859	-1.153175	0.000015
C	0.10685	0.021325	0.000039
C	-0.640273	1.216623	0.00001
C	-2.037673	1.218784	-0.000002
C	-2.712204	0.015587	-0.000012
N	-1.994647	-1.12628	-0.000007
H	-0.132101	2.174132	0.000008
H	-0.207107	-2.145342	0.000029
H	-2.599574	2.143787	-0.00001
H	-3.789431	-0.079263	-0.000027
H	-2.494363	-2.010383	-0.000024
Cu	2.024761	-0.003925	-0.000008
^{2}[(NACu)$_{cyc}$.NH]$^{+\bullet}$			
H	4.845434	-2.22919	0.000035
O	-0.12906	-0.886705	-0.000029
C	-0.399655	0.379189	-0.000007
O	0.47054	1.264796	0.000028
C	-1.850565	0.756148	-0.000027
C	-2.339066	2.060441	-0.000009
C	-2.811756	-0.270273	-0.000066
H	-1.640017	2.889706	0.000021
C	-4.577162	1.173887	-0.000068
H	-5.655055	1.281458	-0.000085
C	4.614172	-1.172425	0.000064
C	5.622946	-0.209476	0.000126
C	3.293713	-0.75725	0.000039
C	5.289889	1.145159	0.000162
H	6.663264	-0.512405	0.000146
H	2.440577	-1.424139	-0.000008
C	3.953249	1.503378	0.000134
H	6.051752	1.913105	0.00021
H	1.964502	0.839806	0.000054
H	3.609205	2.52931	0.000159
N	3.001604	0.55441	0.000075
Cu	-1.786099	-1.938107	-0.000081
N	-4.078588	-0.077119	-0.000085
C	-3.719844	2.271045	-0.00003
H	-4.131271	3.272755	-0.000016
^{2}NAH-Cu-NH$^{+\bullet}$			
O	-1.557039	-2.073584	-0.000012
C	-2.760645	-1.33333	0.000006
O	-3.812473	-1.892633	0.000018
C	-2.46807	0.10867	0.000008
C	-3.496563	1.054473	0.000019
C	-1.136439	0.560146	-0.000003
H	-4.531069	0.728637	0.000028
C	-1.80587	2.751937	0.000012
H	-1.499269	3.792331	0.000015
C	2.042124	-0.37187	-0.000017
C	3.182664	-1.196073	0.000032
C	2.29024	0.997728	-0.000047
C	4.480572	-0.671224	0.000055
H	3.075922	-2.275631	0.000056
H	1.492882	1.73595	-0.000097
C	4.651194	0.695915	0.000026
H	5.350158	-1.315687	0.000094
H	3.68301	2.490636	-0.000049
H	5.61293	1.190052	0.000041
N	3.55412	1.483804	-0.000025
Cu	0.185922	-0.964373	-0.000023
H	-1.769628	-3.020459	-0.000002
C	-3.154469	2.402087	0.000021
H	-3.914815	3.172651	0.00003
N	-0.82329	1.831529	0.000002
^{2}[NAH-Cu-NH]$_{isom.}^{+\bullet}$			
O	-2.20389	0.230611	-1.296247
C	-1.424846	1.324822	-0.915569
O	-1.700238	2.426824	-1.274228
C	-0.21889	0.912396	-0.086909
C	0.066229	1.963989	0.956081
C	-0.159121	-0.49535	0.611377
H	0.311915	2.967421	0.626036
C	-0.475815	0.327156	2.70978
H	-0.745672	0.186101	3.753293

C	1.069753	-0.805022	-0.058202
C	0.990253	0.391006	-0.995293
C	2.241238	-1.469114	0.21184
C	2.32518	1.070449	-1.08722
H	0.629164	0.148633	-2.003497
H	2.332231	-2.318731	0.876104
C	3.431923	0.356678	-0.828996
H	2.413085	2.082391	-1.461259
H	4.259664	-1.417858	-0.128905
H	4.430063	0.743896	-0.98127
N	3.383936	-0.950787	-0.313967
Cu	-1.604546	-1.600283	-0.32344
H	-2.93081	0.546578	-1.860045
C	-0.092042	1.668524	2.256178
H	0.052496	2.430465	3.013373
N	-0.45686	-0.719693	1.952727
^{2}(N-Cu-NH)$_{cyc.}^{+\bullet}$			
C	0.726455	0.719623	0.00005
H	3.586808	2.580497	0.000193
H	4.472602	0.428039	0.000086
C	-0.743897	0.770971	0.000032
C	-1.435456	-0.464785	-0.000046
C	1.537706	1.869225	0.000125
H	1.118945	2.866752	0.000175
C	-1.541297	1.921146	0.000083
H	-1.100165	2.912083	0.000144
C	1.335546	-0.567544	-0.000012
C	2.709123	-0.628802	0.000003
H	3.276062	-1.551117	-0.00004
C	-2.929313	1.793588	0.000054
C	2.908008	1.738556	0.000137
H	-3.566852	2.668726	0.000093
Cu	-0.097572	-1.924486	-0.000105
C	-3.495151	0.521314	-0.000024
H	-4.568623	0.372073	-0.000049
N	3.461423	0.508658	0.000077
N	-2.721355	-0.581045	-0.000072
^{2}A-Ni-ANH^{+}			
C	-0.226748	-4.121009	0
O	-1.282488	-3.4437	0
O	0.894997	-3.559107	0
C	1.308587	2.442131	0
C	0.06967	1.823233	0
C	-1.088976	2.605936	0
C	-0.985422	3.997337	0
C	0.267548	4.577888	0
N	1.366413	3.787721	0
H	-2.056135	2.115708	0
H	2.240765	1.891577	0
H	-1.864722	4.627749	0
H	0.437022	5.646396	0
C	0	0.334587	0
O	-1.112656	-0.263262	0
O	1.053341	-0.366872	0
Ni	-0.110595	-1.925846	0
H	2.281322	4.23114	0
^{3}NA-Ni-NH^{+}			
C	-3.259298	1.209065	-0.485077
C	-2.722588	0.016466	0.024695
C	-3.545132	-0.822284	0.788511
C	-4.855747	-0.429404	1.008979
C	-5.290516	0.779989	0.460866
N	-4.515302	1.588672	-0.272345
H	-3.154442	-1.749594	1.188784
H	-2.641571	1.86914	-1.0852
H	-5.534407	-1.039867	1.591269
H	-6.31118	1.115891	0.616706
C	-1.331677	-0.33912	-0.244021
O	-0.818066	-1.43943	0.197625
O	-0.546793	0.406608	-0.925457
C	2.714185	1.177851	-0.116492
C	2.599872	-0.207971	-0.076309
C	3.73791	-0.905871	0.369051
C	4.911512	-0.243922	0.742697
C	4.955455	1.133044	0.6755
N	3.860628	1.798572	0.250236
H	3.722856	-1.988959	0.433489
H	1.910357	1.832766	-0.431133
H	5.782958	-0.787514	1.083841
H	5.818031	1.727178	0.944881
Ni	0.875963	-0.980245	-0.623616
H	3.898153	2.812633	0.205634
^{3}[NA-Ni-NH]$_{isom.}^{+}$			
C	-1.481262	0.676167	-0.89678
C	-2.3621	0.11917	0.044219
C	-3.000289	0.990694	0.932802
C	-2.690537	2.340494	0.870176
C	-1.733325	2.780483	-0.057435
N	-1.14235	1.973237	-0.936142
H	-3.713635	0.598005	1.647825
H	-1.141941	0.084014	-1.756587
H	-3.163241	3.052657	1.535591
H	-1.446623	3.8266	-0.094965
C	-2.5463	-1.374516	0.14512
O	-3.583185	-1.895527	0.450168
O	-1.404831	-2.041125	-0.091674
C	2.202545	0.982115	-0.386956
C	1.890279	-0.356136	-0.066128
C	4.44739	0.729545	0.406411
H	2.834227	-2.131872	0.800729
H	1.439125	1.620837	-0.822304
H	4.867321	-1.127216	1.137294
H	5.453416	1.062813	0.622515
Ni	0.118442	-1.139578	-0.42815
H	3.70222	2.549164	-0.414081
C	3.471358	1.522975	-0.159048
C	2.925059	-1.095437	0.49874
N	4.145206	-0.54851	0.718646
^{3}[N-Ni-NH.CO$_2$]$^{+}$			
C	2.199813	-0.358765	1.016424
C	1.59293	-0.628117	-0.220592
C	2.237329	-1.547494	-1.061786
C	3.440986	-2.118923	-0.655135
C	3.952378	-1.766712	0.593461
N	3.350052	-0.905836	1.418862
H	1.82463	-1.817767	-2.029965
H	1.745214	0.327467	1.728803
H	3.969861	-2.82349	-1.286337
H	4.882845	-2.198415	0.950075
C	1.038098	3.190329	0.200323
O	0.212847	2.408404	-0.093784
O	1.832957	3.966564	0.489165
C	-2.983839	0.644644	-0.238136
C	-1.895444	-0.219792	-0.214426
C	-2.172092	-1.522117	0.250468
C	-3.450064	-1.917472	0.654231
C	-4.482141	-1.003468	0.599454
N	-4.218667	0.243333	0.157467
H	-1.369269	-2.250187	0.30697
H	-2.930353	1.676881	-0.562212
H	-3.646694	-2.920635	1.009856
H	-5.501375	-1.217098	0.890971
Ni	-0.040989	0.26555	-0.745441

H	-4.981023	0.912958	0.121122
^{4}A-Ni-NH$^{+\bullet}$			
C	-3.326551	0.86568	0.000111
O	-4.44859	1.108522	0.000147
O	-2.17761	0.617562	0.000417
C	2.136254	-0.958626	0.000359
C	0.944114	-0.248718	0.000058
C	1.066005	1.151707	-0.000397
C	2.311449	1.787486	-0.000327
C	3.456676	1.017526	0.000078
N	3.335722	-0.326184	0.000273
H	0.174826	1.77109	-0.000348
H	2.19384	-2.04191	0.000572
H	2.397732	2.866544	-0.000502
H	4.460205	1.420622	0.000181
Ni	-0.831325	-1.298009	-0.000225
H	4.182363	-0.887803	0.000678
^{3}N-Ni-NH^{+}			
C	2.719505	-1.22442	-0.000062
C	4.088291	-1.205034	0.000302
C	4.852233	-0.065222	0.000534
C	4.135071	1.137098	0.000373
C	2.745901	1.097685	0.000006
N	2.035604	-0.049838	-0.000203
H	5.936248	-0.080942	0.00082
H	2.139817	-2.139337	-0.000251
H	4.646716	2.091925	0.000528
H	2.171109	2.016059	-0.000129
C	-2.656652	-1.138575	0.000052
C	-1.868773	0.0142	-0.000178
C	-2.614068	1.217771	-0.000074
C	-4.010651	1.251797	0.000242
C	-4.71145	0.063491	0.000461
N	-4.013006	-1.090449	0.000358
H	-2.090746	2.168638	-0.000249
H	-2.249429	-2.142256	0.000004
H	-4.554548	2.187696	0.000316
H	-5.789899	-0.011668	0.000707
H	-4.528124	-1.964671	0.000515
Ni	0.074437	-0.037007	-0.000475
^{2}Ni-NH$^{+\bullet}$			
C	-0.618586	-1.154846	-0.000003
C	0.135588	0.016352	-0.000008
C	-0.612474	1.213389	-0.000001
C	-2.009248	1.221135	0
C	-2.688408	0.019933	0.000002
N	-1.974172	-1.124081	0
H	-0.101185	2.170111	0.000003
H	-0.190303	-2.149109	0
H	-2.568473	2.147772	0.000001
H	-3.765814	-0.071556	0.000008
H	-2.476991	-2.006273	0.000006
Ni	2.060026	-0.00422	0.000001
^{3}[(NANi)$_{cyc.}$NH]$^{+}$			
H	4.910121	-2.21912	-0.000005
O	-0.174812	-0.9306	-0.000034
C	-0.43591	0.35658	-0.000027
O	0.45575	1.212164	-0.000007
C	-1.878642	0.738402	-0.00004
C	-2.349932	2.050188	-0.000048
C	-2.831156	-0.297475	-0.000044
H	-1.650034	2.878152	-0.000044
C	-4.581868	1.155079	-0.000065
H	-5.659228	1.278171	-0.000075
C	4.655021	-1.167869	0.000035
C	5.641892	-0.182237	0.000117
C	3.325828	-0.782762	0.000005
C	5.278682	1.164551	0.000168
H	6.688719	-0.461813	0.000143
H	2.489379	-1.470094	-0.000057
C	3.934473	1.493082	0.000134
H	6.023092	1.949421	0.000232
H	1.967351	0.786017	0.000029
H	3.566953	2.510804	0.000168
N	3.00466	0.522319	0.000054
N	-4.120586	-0.109387	-0.000056
C	-3.728086	2.2576	-0.000061
H	-4.14146	3.258486	-0.000067
Ni	-1.814741	-1.941568	-0.000037
^{3}NAH-Ni-NH^{+}			
C	1.13754	0.522978	-0.000386
C	2.48653	0.119416	0.000165
C	3.504283	1.077569	0.000424
C	3.134309	2.415641	0.000157
C	1.775783	2.733967	-0.000332
N	0.800525	1.809636	-0.000592
H	4.54475	0.772093	0.000813
H	3.877002	3.20331	0.00033
H	1.456316	3.771428	-0.000521
C	2.804417	-1.315202	0.000367
O	3.859284	-1.868325	0.000503
O	1.60549	-2.083314	0.000341
C	-2.307036	0.968146	0.000191
C	-2.075685	-0.407266	-0.000176
C	-3.228214	-1.215022	-0.000194
C	-4.519416	-0.673567	0.00027
C	-4.671843	0.695631	0.000564
N	-3.56452	1.469529	0.000462
H	-3.136358	-2.296253	-0.000539
H	-1.497373	1.69443	0.000191
H	-5.397631	-1.306177	0.000351
H	-5.627174	1.202152	0.000816
Ni	-0.178436	-0.977486	-0.000515
H	1.842639	-3.024274	0.00033
H	-3.680214	2.4781	0.000505
^{3}[NAH-Ni-NH]$^{+}$			
C	-1.172773	0.714211	0.022837
C	-0.642924	-0.692054	-0.21895
C	-1.685367	-1.442388	-1.018251
C	-2.960886	-0.963822	-1.125195
C	-3.334235	0.292463	-0.59262
N	-2.361573	1.128202	-0.099056
H	-1.416262	-2.401909	-1.44631
H	-3.712792	-1.545409	-1.646158
H	-4.345467	0.671994	-0.627588
C	-0.377935	-1.335085	1.174297
O	0.698997	-1.344335	1.712306
O	-1.496705	-1.833119	1.70964
C	2.654352	0.885115	0.042703
C	1.308382	0.824275	-0.227107
C	0.7398	-0.408514	-0.900445
C	1.710331	-1.541715	-1.027156
C	3.013821	-1.376741	-0.72607
N	3.470651	-0.173218	-0.225257
H	0.467632	-0.103622	-1.928572
H	3.138603	1.735963	0.505249
H	1.377819	-2.495186	-1.419501
H	3.758658	-2.152194	-0.837933
Ni	0.024	2.056033	0.259617
H	-1.290451	-2.181974	2.592392
H	4.452974	-0.096303	0.009502
^{3}(N-Ni-NH)$_{cyc.}$$^{+}$			

C	0.731301	0.688297	0.000048
H	3.588893	2.555648	0.000193
H	4.481828	0.405853	0.000086
C	-0.741679	0.741949	0.00003
C	-1.438467	-0.493852	-0.000048
C	1.542549	1.839151	0.000124
H	1.123044	2.836103	0.000174
C	-1.516414	1.908877	0.000081
H	-1.061012	2.893187	0.000142
C	1.346425	-0.600123	-0.000014
C	2.719939	-0.655549	0.000002
H	3.290238	-1.576056	-0.000041
C	-2.903077	1.799161	0.000054
C	2.912553	1.71162	0.000137
H	-3.530607	2.681553	0.000092
C	-3.481785	0.530853	-0.000024
H	-4.559214	0.405733	-0.000048
N	3.470667	0.483428	0.000076
N	-2.744738	-0.593896	-0.000073
Ni	-0.122955	-1.937537	-0.000106
^{1}NA-Ni-NH^{+}			
C	3.004362	1.38739	0.000125
C	2.701512	0.017338	0.000048
C	3.752823	-0.909633	0.000017
C	5.05026	-0.423838	0.000064
C	5.244785	0.96017	0.00014
N	4.248293	1.854354	0.00017
H	3.542854	-1.972249	-0.000043
H	2.206604	2.123252	0.000151
H	5.900257	-1.094395	0.000042
H	6.249599	1.371254	0.000177
C	1.320234	-0.440157	0.000001
O	0.9743	-1.667282	-0.000066
O	0.311995	0.378906	0.000023
C	-2.588156	1.186261	0.000017
C	-2.532005	-0.203015	-0.000055
C	-3.767494	-0.874511	-0.000114
C	-4.981458	-0.180381	-0.000099
C	-4.966491	1.198886	-0.000025
N	-3.775179	1.834699	0.00003
H	-3.804142	-1.96029	-0.000172
H	-1.704352	1.811857	0.000066
H	-5.929522	-0.702286	-0.000144
H	-5.853941	1.816497	-0.000008
H	-3.770517	2.850237	0.000084
Ni	-0.852472	-1.073975	-0.000068
^{1}[NA-Ni-NH]$_{isom.}^{+}$			
C	-1.320145	0.730741	0.722113
C	-2.424412	0.04552	0.190991
C	-3.387307	0.792023	-0.496296
C	-3.171615	2.151657	-0.660367
C	-1.993151	2.725115	-0.156433
N	-1.085431	2.039083	0.534935
H	-4.269437	0.299624	-0.888388
H	-0.666648	0.237664	1.447767
H	-3.889102	2.770523	-1.185289
H	-1.787013	3.77922	-0.311399
C	-2.508379	-1.457193	0.288903
O	-3.536472	-2.059772	0.425563
O	-1.306306	-2.037112	0.131711
C	3.101505	-1.069621	-0.312068
C	1.970026	-0.286427	-0.104502
C	2.216592	1.065806	0.218323
C	3.512867	1.579519	0.318229
C	4.586291	0.742268	0.097427
N	4.349318	-0.550692	-0.209169
H	1.379907	1.735848	0.399626
H	3.072094	-2.12365	-0.560819
H	3.690861	2.617632	0.567306
H	5.621323	1.051031	0.154807
Ni	0.14663	-1.034458	-0.236863
H	5.143772	-1.163174	-0.367911
^{1}[N-Ni-NH.CO$_2$]$^{+}$			
C	-3.023778	-2.109464	-0.128984
O	-4.170548	-2.11258	-0.129097
O	-1.849575	-2.128435	-0.128817
Ni	-0.105286	-1.044353	-0.056248
C	1.66059	-0.450239	-0.033885
C	2.617728	-1.149884	0.730457
C	2.158041	0.601711	-0.802065
C	3.975422	-0.816709	0.707358
H	2.310539	-1.976208	1.363809
H	1.536076	1.236214	-1.418499
H	4.699157	-1.361672	1.29943
H	3.791042	1.672758	-1.390655
C	-0.809804	0.670552	0.097414
C	-0.964636	1.307791	1.330558
C	-1.331199	1.288527	-1.045303
C	-1.660951	2.514887	1.373843
H	-0.562123	0.882425	2.243235
H	-1.230603	0.842282	-2.031948
H	-1.814195	3.035956	2.311849
C	-2.149079	3.047077	0.180593
H	-2.685717	3.990817	0.174437
C	4.397775	0.230113	-0.084558
H	5.424614	0.558336	-0.166101
N	3.477549	0.900804	-0.810318
N	-1.989042	2.453897	-1.003948
^{2}A-Ni-NH$^{+\bullet}$			
C	3.993513	0.007135	0.000833
O	2.82267	-0.024626	-0.000234
O	5.140589	0.036483	0.001834
C	-1.88317	-1.150971	-0.000212
C	-1.108911	0.009894	-0.000261
C	-1.85719	1.210432	-0.000339
C	-3.253193	1.232701	-0.000306
C	-3.944785	0.038644	-0.000232
N	-3.238644	-1.110147	-0.000185
H	-1.341697	2.165356	-0.000412
H	-1.468514	-2.151335	-0.000209
H	-3.803317	2.164796	-0.000335
H	-5.022732	-0.044047	-0.000226
H	-3.747806	-1.988245	-0.000173
Ni	0.809676	-0.019906	-0.000252
^{1}N-Ni-NH^{+}			
C	1.762152	0.416891	1.188811
C	1.430764	-0.256296	0.005782
C	2.315125	-0.212647	-1.077684
C	3.523643	0.463895	-0.913367
C	3.771298	1.090966	0.307325
N	2.915824	1.073397	1.333393
H	2.088882	-0.692636	-2.024585
H	1.095151	0.425224	2.045165
H	4.248876	0.513161	-1.717049
H	4.693879	1.640748	0.46631
C	-1.441428	0.95592	-0.616083
C	-1.411065	-0.323345	-0.06544
C	-2.614687	-0.779651	0.508767
C	-3.771777	0.003877	0.513421
C	-3.735148	1.261555	-0.05239
N	-2.576611	1.692394	-0.594647
H	-2.666163	-1.762146	0.967667
H	-0.586019	1.430908	-1.075

H	-4.691757	-0.354486	0.956636
H	-4.578509	1.93698	-0.09089
H	-2.553747	2.620311	-1.006837
Ni	0.057202	-1.458771	-0.088839
^{1}[(NANi)$_{cyc.}$.NH]$^{+}$			
H	4.855945	-2.255506	0.000043
O	-0.233402	-0.83897	-0.000031
C	-0.440076	0.458077	-0.000001
O	0.480041	1.28046	0.00004
C	-1.877088	0.820676	-0.000021
C	-2.485068	2.070261	-0.000001
C	-2.717406	-0.296579	-0.000067
H	-1.8883	2.975824	0.000034
C	-4.614455	0.927379	-0.000075
H	-5.698175	0.930222	-0.000097
C	4.625749	-1.19853	0.000068
C	5.635359	-0.236159	0.000121
C	3.306034	-0.782332	0.000048
C	5.30372	1.118789	0.000152
H	6.675352	-0.540182	0.000137
H	2.454763	-1.451136	0.000009
C	3.967695	1.478878	0.00013
H	6.066337	1.885972	0.000193
H	1.986289	0.817921	0.000063
H	3.623889	2.504831	0.000152
N	3.015513	0.52997	0.00008
N	-4.009399	-0.281155	-0.000093
C	-3.883536	2.114728	-0.000029
H	-4.407773	3.062134	-0.000015
Ni	-1.771778	-1.859101	-0.000088
^{1}NAH-Ni-NH^{+}			
C	0.993011	0.502109	-0.000193
C	2.36238	0.147045	0.000144
C	3.331695	1.150709	0.000335
C	2.914044	2.475192	0.000139
C	1.546387	2.733575	-0.000235
N	0.617343	1.761643	-0.000359
H	4.382133	0.881104	0.000613
H	3.625174	3.291062	0.000254
H	1.175846	3.753447	-0.000434
C	2.74862	-1.266558	0.000158
O	3.821401	-1.781295	0.000459
O	1.570617	-2.0495	-0.000463
C	-2.240039	1.06733	0.000151
C	-1.851655	-0.267411	0.000215
C	-2.901966	-1.208116	0.000221
C	-4.246833	-0.822994	0.000283
C	-4.558004	0.519565	0.000195
N	-3.545726	1.41477	-0.000035
H	-2.691136	-2.274985	0.000039
H	-1.505526	1.867211	-0.000095
H	-5.043465	-1.55543	-0.000056
H	-5.565028	0.912507	0.00011
Ni	-0.129251	-1.001998	-0.000189
H	1.795793	-2.993021	-0.000665
H	-3.778079	2.402826	-0.000146

^{1}[NAH-Ni-NH]$_{isom.}$$^{+}$			
C	-0.820928	-0.907648	0.134015
C	-0.703287	0.585197	-0.053647
C	-1.088473	1.250308	1.256968
C	-1.814045	0.591966	2.187297
C	-2.273038	-0.736177	1.874581
N	-1.736863	-1.446477	0.901329
H	-0.893572	2.31294	1.342119
H	-2.156993	1.075932	3.092909
H	-3.085804	-1.187267	2.436688
C	-1.697237	1.190699	-1.104435
O	-1.773444	2.366485	-1.306396
O	-2.39367	0.239783	-1.740787
C	2.758477	-0.560521	0.092525
C	1.477852	-0.504214	-0.343261
C	0.756105	0.823527	-0.560485
C	1.513151	1.951868	0.115163
C	2.796801	1.8064	0.474283
N	3.458005	0.588042	0.38265
H	0.702653	1.034464	-1.638465
H	3.294806	-1.487393	0.260672
H	1.050243	2.926385	0.200003
H	3.383531	2.623097	0.873461
Ni	0.432972	-2.009685	-0.496869
H	-2.976316	0.662335	-2.395706
H	4.41488	0.521158	0.692224
^{1}(N-Ni-NH)$_{cyc.}$$^{+}$			
C	0.742665	0.788677	0.000054
H	3.75908	2.365189	0.000187
H	4.431337	0.14289	0.000074
C	-0.710593	0.871086	0.000037
C	-1.297373	-0.409983	-0.000042
C	1.647031	1.85854	0.000127
H	1.315743	2.888954	0.000179
C	-1.584323	1.958775	0.000082
H	-1.222446	2.981482	0.000144
C	1.219535	-0.559	-0.000013
C	2.582634	-0.75181	-0.000003
H	3.064324	-1.721189	-0.00005
C	-2.958373	1.703257	0.000047
C	3.000766	1.594163	0.000133
H	-3.671156	2.518112	0.00008
C	-3.417402	0.387096	-0.000033
H	-4.477122	0.15862	-0.000063
N	3.432437	0.317197	0.000068
N	-2.56828	-0.663848	-0.000076
Ni	-0.164152	-1.841154	-0.000101